

**DTIC FILE COPY**

4

**RADC-TR-89-88**  
**In-House Report**  
**June 1989**



**AD-A223 110**

# **BACKSCATTER ENHANCEMENT IN SCATTERING FROM ROUGH SURFACES**

**Robert J. Papa and Margaret B. Woodworth**

**DTIC**  
**ELECTE**  
**JUN 13 1990**  
**S B D**  
*Ec*

**APPROVED FOR PUBLIC RELEASE; DISTRIBUTION UNLIMITED.**

**ROME AIR DEVELOPMENT CENTER**  
**Air Force Systems Command**  
**Griffiss Air Force Base, NY 13441-5700**

**90 06 12 138**

This report has been reviewed by the RADC Public Affairs Division (PA) and is releasable to the National Technical Information Service (NTIS). At NTIS it will be releasable to the general public, including foreign nations.

RADC-TR-89-88 has been reviewed and is approved for publication.

APPROVED:



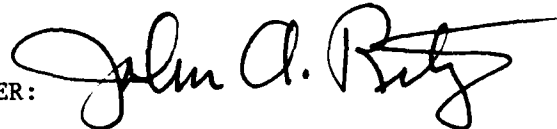
J. LEON POIRIER  
Chief, Applied Electromagnetics Division

APPROVED:



JOHN K. SCHINDLER  
Director of Electromagnetics

FOR THE COMMANDER:



JOHN A. RITZ  
Directorate of Plans & Programs

If your address has changed or if you wish to be removed from the RADC mailing list, or if the addressee is no longer employed by your organization, please notify RADC (EECE ) Hanscom AFB MA 01731-5000. This will assist us in maintaining a current mailing list.

Do not return copies of this report unless contractual obligations or notices on a specific document require that it be returned.

REPORT DOCUMENTATION PAGE			Form Approved OMB No 0704-0188	
Public reporting burden for this collection of information is estimated to average 1 hour per response, including the time for reviewing instructions, searching existing data sources, gathering and maintaining the data needed, and completing and reviewing the collection of information. Send comments regarding this burden estimate or any other aspect of this collection of information, including suggestions for reducing this burden, to Washington Headquarters Services, Directorate for Information Operations and Reports, 1215 Jefferson Davis Highway, Suite 1204, Arlington, VA 22202-4302, and to the Office of Management and Budget, Paperwork Reduction Project (0704-0188), Washington, DC 20503.				
1. AGENCY USE ONLY (Leave blank)	2. REPORT DATE JUN 89	3. REPORT TYPE AND DATES COVERED In-house JUL 88 - JAN 89		
4. TITLE AND SUBTITLE Backscatter Enhancement in Scattering from Rough Surfaces		5. FUNDING NUMBERS PE-61102F PR-2305 TA-J4 WU-09		
6. AUTHOR(S) Papa, Robert J. and Woodworth,* Margaret B.				
7. PERFORMING ORGANIZATION NAME(S) AND ADDRESS(ES) Rome Air Development Center RADC/EECE Hanscom AFB Massachusetts 01731-5000		8. PERFORMING ORGANIZATION REPORT NUMBER RADC-TR-89-88		
9. SPONSORING / MONITORING AGENCY NAME(S) AND ADDRESS(ES)		10. SPONSORING / MONITORING AGENCY REPORT NUMBER		
11. SUPPLEMENTARY NOTES *ARCON Corporation				
12a. DISTRIBUTION / AVAILABILITY STATEMENT Approved for Public Release; Distribution Unlimited		12b. DISTRIBUTION CODE		
13. ABSTRACT (Maximum 200 words) Stealth technology has advanced to the point where radar target cross sections are so small there is a great need to determine mean clutter cross sections and clutter variability with great accuracy. Established clutter prediction techniques result in forward scatter values that exceed backscatter. There is some new experimental data on light scattering from rough metallic surfaces which shows there is an enhancement of backscattering in the antispecular direction under some conditions. This unusual result has been addressed by several theoretical analyses with varying success at confirmation. In this report an integral form of a physical optics representation is used to simulate the experimental conditions. For a one-dimensional surface height variation this model predicts enhanced backscatter at optical frequencies. Additional calculations for the more significant radar case of microwave frequencies and a dielectric surface again predict an increase in backscatter for large or intermediate surface slope conditions. <i>W. Woodworth</i>				
14. SUBJECT TERMS Rough Surface Scattering, Radar Clutter, Bistatic Clutter. <i>W. Woodworth</i>			15. NUMBER OF PAGES 44	
			16. PRICE CODE	
17. SECURITY CLASSIFICATION OF REPORT UNCLASSIFIED	18. SECURITY CLASSIFICATION OF THIS PAGE UNCLASSIFIED	19. SECURITY CLASSIFICATION OF ABSTRACT UNCLASSIFIED	20. LIMITATION OF ABSTRACT SAR	

## Preface

This report presents the combined results of the authors individual efforts. Dr. Papa formulated the theory and analyzed the results (Sections 1, 2, and 5) while Mrs. Woodworth developed the mathematical techniques (described in Section 2) that permitted the numerical results to be obtained (Sections 3 and 4).



Accession For	
NTIS GRA&I	<input checked="" type="checkbox"/>
DTIC TAB	<input type="checkbox"/>
Unannounced	<input type="checkbox"/>
Justification	
By	
Distribution/	
Availability Codes	
Dist	Avail and/or Special
A-1	

## Contents

1. INTRODUCTION	1
1.1 Discussion Of The Experiment	2
1.2 Summary Of Analytical Efforts	2
2. $\sigma^0$ MODELS USED IN THIS REPORT	4
2.1 Physical Optics Triple Integral Solution	4
2.2 Small Slope Approximations	6
2.3 Geometrical Optics Solution	7
2.4 RMS Slope Model	7
3. THE THEORETICAL AND EXPERIMENTAL RESULTS FOR METALLIC ROUGH SURFACES AT OPTICAL FREQUENCIES	8
4. THE THEORETICAL RESULTS FOR DIELECTRIC ROUGH SURFACES AT RADIO FREQUENCIES	23
5. SUMMARY AND CONCLUSIONS	33
REFERENCES	35

## Illustrations

1. The Normalized Cross Section $\sigma^0$ vs Scattering Angle for an Aluminum Surface with Different Roughness Conditions	10
2. The Normalized Cross Section $\sigma^0$ vs Scattering Angle for an Aluminum Surface, $\theta_i = 70^\circ$ , $\sigma/T = 0.556$	11
3. The Normalized Cross Section $\sigma^0$ vs Scattering Angle for an Aluminum Surface, $\theta_i = 70^\circ$ , $\sigma/T = 1.11$	12
4. The Normalized Cross Section $\sigma^0$ vs Scattering Angle for an Aluminum Surface, $\theta_i = 60^\circ$ , $\sigma/T = 1.11$	13
5. The Normalized Cross Section $\sigma^0$ vs Scattering Angle for an Aluminum Surface, $\theta_i = 70^\circ$ , $\sigma/T = 0.5$	14
6. The Normalized Cross Section $\sigma^0$ vs Scattering Angle for an Aluminum Surface, $\theta_i = 70^\circ$ , $\sigma/T = 0.5$ with Large Standard Deviation in Surface Height	15
7. The Normalized Intensity vs Scattering Angle for a Gold Diffuser, Experimental Data	16
8. The Normalized Cross Section $\sigma^0$ vs Scattering Angle for a Gold Surface, $\theta_i = 70^\circ$ , $\sigma/T = 0.109$	17
9. The Normalized Cross Section $\sigma^0$ vs Scattering Angle for a Gold Surface, $\theta_i = 70^\circ$ , $\sigma/T = 0.216$	18
10. The Normalized Cross Section $\sigma^0$ vs Scattering Angle for a Gold Surface, $\theta_i = 70^\circ$ , $\sigma/T = 0.432$	19
11. The Normalized Cross Section $\sigma^0$ vs Scattering Angle for a Gold Surface, $\theta_i = 70^\circ$ , $\sigma/T = 1.135$	20

## Illustrations (Contd.)

12. The Normalized Cross Section $\sigma^0$ vs Scattering Angle for a Gold Surface, $\theta_1 = 70^\circ$ , Two Correlation Lengths $\sigma/T_{\text{short}} = 0.4504$	21
13. The Normalized Cross Section $\sigma^0$ vs Scattering Angle for a Gold Surface, $\theta_1 = 70^\circ$ , Two Correlation Lengths $\sigma/T_{\text{short}} = 1.14$	22
14. The Normalized Cross Section $\sigma^0$ vs Scattering Angle for a Gold Surface, $\theta_1 = 70^\circ$ , Two Correlation Lengths $\sigma/T_{\text{short}} = 2.27$	23
15. The Normalized Cross Section $\sigma^0$ vs Scattering Angle for a Dielectric Surface with Different Roughness Conditions	25
16. The Normalized Cross Section $\sigma^0$ vs Scattering Angle for a Dielectric Surface, $\theta_1 = 60^\circ$	26
17. The Normalized Cross Section $\sigma^0$ vs Scattering Angle for a Dielectric Surface, $\theta_1 = 75^\circ$	27
18. The Normalized Cross Section $\sigma^0$ vs Scattering Angle for a Lossy Dielectric Surface, $\theta_1 = 40^\circ$ , $\sigma/T = 0.6$	28
19. The Normalized Cross Section $\sigma^0$ vs Scattering Angle for a Lossy Dielectric Surface, $\theta_1 = 40^\circ$ , $\sigma/T = 0.833$	29
20. The Normalized Cross Section $\sigma^0$ vs Scattering Angle for a Lossy Dielectric Surface, $\theta_1 = 40^\circ$ , $\sigma/T = 1.25$	30
21. The Normalized Cross Section $\sigma^0$ vs Scattering Angle for a Lossy Dielectric Surface, $\theta_1 = 40^\circ$ , $\sigma/T = 1.67$	31
22. The Normalized Cross Section $\sigma^0$ vs Scattering Angle for a Lossy Dielectric Surface, $\theta_1 = 75^\circ$ , $\sigma/T = 1.25$	32

# Backscatter Enhancement in Scattering from Rough Surfaces

## 1. INTRODUCTION

Stealth technology has advanced to the point where typical radar target cross sections are so small that the design of future radar systems will require very high sensitivity. The small target cross section combined with clutter variability in space and time will require radar receivers with dynamic ranges of 90 dB (over a 1 percent bandwidth). Hence, there is now a need for accurate models to predict radar clutter power levels in various environmental situations.

As a result of recent experimental data at optical frequencies,<sup>1</sup> there is a question whether the traditional clutter prediction models are accurate under some conditions. This report shows that a one-dimensional physical optics integral representation confirms the new data. The model is then applied at microwave frequencies. The results show that the conventional model for mean clutter cross section can underestimate the value by as much as 10 dB for very rough surfaces.

---

(Received for Publication 16 June 1989)

<sup>1</sup> Mendez, E.R. and O'Donnell, K.A. (1987) Observation of depolarization and backscattering enhancement in light scattering from Gaussian random surfaces, *Optics Communications*, 61(2):91-95.



## 1.1 Discussion of the Experiment

In January 1987, Mendez and O'Donnell<sup>1</sup> first reported experimental observations of enhanced backscattering in the antisp specular direction when light was scattered from rough metallic surfaces. This initial work was further corroborated in a paper<sup>2</sup> which reported on light scattering from metallic surfaces under a variety of rough surface conditions. O'Donnell and Mendez<sup>2</sup> found that when the surface slopes are small, the diffuse scattering often agrees with the physical optics (PO) theory of Beckmann and Spizzichino<sup>3</sup> (conventional model) when the angle of incidence is not too large. However, when the surface slopes became larger, the theory of Reference 3 departs from the experimental data. Mendez and O'Donnell speculate that multiple scattering is a factor.

## 1.2 Summary of Analytical Efforts

There are a large number of theoretical approaches<sup>4, 5, 6, 7, 8, 9, 10</sup> to scattering from rough surfaces. Each approach, even the more rigorous theories which include multiple scattering,<sup>6,7,9,10</sup> are based upon certain restrictive assumptions. To date, only References 8, 9, and 10 appear to predict backscatter enhancement in the antisp specular direction and as Flood<sup>11</sup> points out, of these only Bahar's<sup>8</sup> approach shows any agreement with the

---

<sup>2</sup> O'Donnell, K.A. and Mendez, E.R. (1987) Experimental study of scattering from characterized random surfaces, *Journal Optical Society of America*, **4**:1194-1205.

<sup>3</sup> Beckmann, P. and Spizzichino, A. (1963) *The Scattering of Electromagnetic Waves From Rough Surfaces*, Pergamon Press, New York.

<sup>4</sup> Desanto, J.A. and Brown, G.S. (1986) Analytical techniques for multiple scattering from rough surfaces, E. Wolf, *Progress In Optics*, **XXIII**, Elsevier Science Publishers.

<sup>5</sup> Ruck, G.T., Barrick, D.E., Stuart, W.D. and Krickbaum, C.T. (1970) *Radar Cross Section Handbook*, **2**, Plenum Press.

<sup>6</sup> Brown, G.S. (1984) Application of the integral equation method of smoothing to random surface scattering, *IEEE Trans. on Antennas and Propagation*, **AP-32**(12):1308-1312.

<sup>7</sup> Nieto-Vesperinas, M. and Garcia, N. (1981) A detailed study of the scattering of scalar waves from random rough surfaces, *Opt. Acta*, **28**:1651-1672.

<sup>8</sup> Bahar, E. (1987) Review of the full wave solutions for rough surface scattering and depolarization: Comparisons with geometric and physical optics, perturbation and two-scale hybrid solutions, *J. Geophys. Res.*, **92**(C5):5209-5224.

<sup>9</sup> Celli, V., Maraduden, A.A., Marvin, A.M. and McGurn, A.R. (1985) Some aspects of light scattering from a randomly rough metal surface, *J. Opt. Soc. America*, **A2**:2225.

<sup>10</sup> McGurn, A.R., Maraduden, A.A. and Celli, V. (1985) Localization effects in the scattering of light from a randomly rough grating, *Phys. Rev.*, **B31**:4866.

<sup>11</sup> Flood, W. (1987) Wave Propagation: Although Electromagnetics is a Mature Science, New Problems are Challenging the Theoreticians, R & D Roundup, *Microwaves and RF*, **65**.

experimental data of Mendez and O'Donnell. This is significant in terms of the original experiment since although multiple levels of roughness appear in the model, Bahar does not include multiple scattering in his formalism.

Thorsos and Ishimaru<sup>12</sup> have examined the accuracy of Bahar's<sup>8</sup> full-wave solution using a one-dimensional surface with a Gaussian roughness spectrum. The normalized bistatic scattering cross section  $\sigma^0$  is calculated by solving an integral equation for the scattered field and then using a Monte Carlo technique to ensemble average over the surface heights. Based upon comparisons with this rigorous mathematical simulation, the full-wave solution was found to agree closely with the Kirchhoff solution (PO), except for small grazing incident and scattering angles. However, Thorsos and Ishimaru<sup>12</sup> found that the full-wave solution does not reduce to the first order perturbation solution (Ruck et al)<sup>5</sup> as the rms surface height and slope become small. Thorsos and Ishimaru<sup>12</sup> conclude that the full-wave method is not an improvement over the Kirchhoff approximation for the case where the incident and scattering angles are not close to 90° (grazing).

Brown<sup>13</sup> has derived an expression for the normalized cross section of a rough surface  $\sigma^0$  starting with the expression for the far field approximation for the scattered field and making the Kirchhoff approximation for the surface current density. Brown assumes Gaussian distributed surface heights and a Gaussian correlation function, and retains terms in the expression for the scattered field that depend upon the surface slopes. He shows that for small, intermediate, and large values of  $kT$ , there is enhancement in the backscatter (antispecular) direction, except for  $\theta_i = 0^\circ$ . Here,  $\theta_i$  = angle of incidence with respect to normal,  $k = 2\pi/\lambda$ ,  $\lambda$  = em wavelength and  $T$  = surface correlation length.

In this report, a model for  $\sigma^0$  is used that is described in Papa and Woodworth.<sup>14</sup> It is assumed that the surface current density is given by the Kirchhoff approximation. Several conditions are placed on the surface. First, the surface heights  $z$  are a random stationary stochastic process and are a function of only one coordinate  $x$  (one-dimensional roughness). The heights are assumed to be Gaussian with a Gaussian correlation. Arbitrary surface slopes are allowed so the surface heights and slopes are not decorrelated. Under these conditions the expression for  $\sigma^0$  reduces to a triple integral, which may be evaluated numerically. For intermediate or large rms surface slopes, this exact physical optics (PO) model predicts enhanced backscatter.

---

<sup>12</sup> Thorsos, E.I. and Ishimaru, A. (1988) An examination of the full-wave method for rough surface scattering, URSI Radio Science Session B/F-1, Jan. 1988, Univ. of Colorado, Boulder, CO.

<sup>13</sup> Brown, G.S. (1988) Enhanced Backscatter from the Kirchhoff Approximation, Private Communication.

<sup>14</sup> Papa, R.J. and Woodworth, M.B. (1988) *The numerical evaluation of a physical optics normalized cross section for a rough surface*, RADC-TR-87-280, ADA198919.

## 2. $\sigma^0$ MODELS USED IN THIS REPORT

A number of different models that incorporate different assumptions are compared in this report in terms of their ability to predict enhanced backscatter. This section will describe these models and their respective differences.

### 2.1 Physical Optics Triple Integral Solution

In the report by Papa and Woodworth,<sup>14</sup> a general expression for the normalized cross section  $\sigma^0$  is derived for a rough surface whose random heights,  $z$ , have only a one-dimensional variation  $z = z(x)$ . The surface current density is assumed to be given by the Kirchhoff approximation. This physical optics (PO) result is valid only under the assumption  $T \gg \lambda$  (Papa and Lennon).<sup>15</sup> The scattering is assumed to take place in the plane of incidence (azimuthal angle,  $\phi = 0^\circ$ ), the incident field is horizontally polarized and there is no shadowing.

The general PO expression for  $\sigma^0$  for a one-dimensional rough surface involves a six-fold integral over the variables  $x_1$ ,  $x_2$ ,  $z_1$ ,  $z_2$ ,  $\mu_1$ , and  $\mu_2$ , where  $x_1$  and  $x_2$  are two points on the surface,  $z_1$  and  $z_2$  are the heights, and  $\mu_1$  and  $\mu_2$  are the slopes at the two points. By assuming that the random rough surface is a stationary stochastic process, the six-fold integral reduces to a four-fold integral over the variables  $\xi$ ,  $\tau$ ,  $\mu_1$  and  $\mu_2$ , where  $\xi = z_1 - z_2$  and  $\tau = x_1 - x_2$ . If the trivariate distribution function for the heights  $z$  and slopes  $\mu_1$  and  $\mu_2$  is assumed to be Gaussian, the integration over  $\xi$  can be accomplished analytically. The remaining expression for  $\sigma^0$  then reduces to a triple integral (II), which may be evaluated numerically using a modified Gaussian quadrature technique.<sup>14</sup>

The expression for  $\sigma^0$  was written as:

$$\sigma^0 = 2 \left( \frac{k}{4\pi^2} \right) \int_0^\infty d\tau \cos |v_x \tau| W(\tau) \quad (1)$$

where

$$v_x = k(\sin \theta_i - \sin \theta_s) \\ W(\tau) = G(\tau) - H$$

---

<sup>15</sup> Papa, R.J. and Lennon, J.F. (1988) Conditions for the validity of physical optics in rough surface scattering, *IEEE Trans. on Antennas and Propagation*, **36**(5):647-650.

and

$$G(\tau) = 2 \int_{-\infty}^{\infty} d\mu_2 F(\mu_2) \int_{-\infty}^{\infty} d\mu_1 F(\mu_1) \int_0^{\infty} d\xi \cos(v_z \xi) p_3(\mu_1, \mu_2, \xi, \tau). \quad (2)$$

Here,  $p_3$  = trivariate distribution function in  $\xi$ ,  $\mu_1$  and  $\mu_2$  and  $v_z = -k(\cos \theta_1 + \cos \theta_s)$ . Also,  $F(\mu)$  is a complicated function of the slopes  $\mu$ , the angle of incidence  $\theta_i$ , the scattering angle  $\theta_s$  and the Fresnel reflection coefficient, and is given in Reference 14, as is the function  $H$ . There, it is shown that

$$I = \int_0^{\infty} d\xi \cos(v_z \xi) p_3 = e^{-C} \cos(v_z B) e^{-v_z^2/4A} \quad (3)$$

where

$$A = \frac{M_{11}}{(2|R|)}$$

$$B = \left( \frac{M_{12}}{M_{11}} \right) (\mu_1 + \mu_2)$$

$$C = \left( \frac{\sigma^2}{T^2} \right) \left( \frac{1}{M_{11}} \right) [\mu_1^2 + \mu_2^2 + 2\bar{F}\mu_1\mu_2]$$

$$\bar{F} = -\exp\left(\frac{-\tau^2}{T^2}\right) \left[ 1 - \frac{2\tau^2}{T^2} \right]$$

$\sigma$  = standard deviation in surface heights and  $M_{ij}$  is the co-factor of the covariance matrix  $R_{ij}$ . The function  $W(\tau)$  in Eq. (1) has singularities in  $\tau$ , but they can be shown to be integrable. This result forms the basic expression to be used in the comparisons of this report.

## 2.2 Small Slope Approximations

Beckmann and Spizzichino<sup>3</sup> show that if the rms surface slopes ( $\sqrt{2} \sigma/T$ ) are small, the PO expression for  $\sigma^o$  for a one-dimensional rough surface reduces to a single integral over  $\tau$ :

$$\sigma^o = \frac{2kF^2(\mu_{sp})}{4\pi^2} \int_0^\infty d\tau \cos|v_x \tau| \left[ \chi_2 - \chi_1^2 \right] \quad (4)$$

where

$$\chi_2 = \exp \left[ -\sigma^2 v_z^2 (1 - \zeta) \right]$$

$$\zeta = \exp \left( -\frac{\tau^2}{T^2} \right)$$

$$\chi_1 = \exp \left[ -\frac{v_x^2 \sigma^2}{2} \right]$$

and  $\mu_{sp}$  is the slope of a facet that gives rise to scattering in the specular direction. This simplification is called physical optics,  $F(\mu_{sp})$ . There are other, alternative, simplified forms for  $\sigma^o$ , which may be obtained from the triple integral given by Eqs. (1), (2), and (3). Another simplification occurs for  $\sigma/T < 1$ ; in the Gaussian trivariate distribution function in Eq. (2), the heights decorrelate from the slopes so that

$$G(\tau) \rightarrow 2 \int_{-\infty}^{\infty} d\mu_2 F(\mu_2) \int_{-\infty}^{\infty} d\mu_1 F(\mu_1) I(\tau) \quad (5)$$

with  $I(\tau)$  given by Eq. (3). Examination of this result shows that now one can separately perform the remaining integrations over  $\mu_1$ ,  $\mu_2$  and  $\tau$ . This simplification into three separate integrations is called physical optics with the F integral (PO, F INT).

Another simplification occurs for small rms slopes ( $\sigma/T < 1$ ); one argues that most of the contributions to the  $\mu_1$  and  $\mu_2$  integrations in Eq. (5) come at  $\mu_1 = 0$  and  $\mu_2 = 0$ , so that then

$$G(\tau) \rightarrow 2 F^2(0) I(\tau). \quad (6)$$

This simplification is called PO,  $F(0)$ .

### 2.3 Geometrical Optics Solution

$$\text{Let } \Sigma = -v_z \sigma = \left( \frac{2\pi\sigma}{\lambda} \right) (\cos \theta_1 + \cos \theta_s),$$

where  $\Sigma$  is the Rayleigh parameter. For the geometrical optics (GO) limit,  $\lambda \rightarrow 0$  and  $\Sigma > 1$  so that Eq. (4) may be evaluated for  $\sigma^o$  using the method of stationary phase<sup>3</sup>:

$$\sigma^o = \frac{k F^2(\mu_{sp})}{4\pi^2} \left( \frac{T\sqrt{\pi}}{\Sigma} \right) \exp \left( -\frac{v^2 T^2}{4\Sigma^2} \right). \quad (7)$$

### 2.4 RMS Slope Model

In order to make the exact PO, triple integral model more flexible and perhaps improve our ability to match the theoretical model to experimental data, we may introduce a two correlation lengths surface roughness scattering model, as follows. In Eqs. (1) through (5), let  $\sigma/T \rightarrow \sigma/T_{\text{short}}$ , where  $\sqrt{2} \sigma/T_{\text{short}}$  represents the rms slopes of the scattering facets. This implies that, everywhere,

$$\frac{T}{\Sigma} \rightarrow \left\{ \frac{\lambda}{\left[ \left( \frac{\sigma}{T} \right) 2\pi (\cos \theta_1 + \cos \theta_s) \right]} \right\}.$$

However, in the expressions containing the correlation function

$$R = \sigma^2 \exp \left( -\frac{\tau^2}{T^2} \right)$$

let  $T \rightarrow T_{\text{long}}$ , where  $T_{\text{long}}$  represents the distance one must travel from one point on the surface to a second point for statistical decorrelation to occur.  $T_{\text{long}}$  is the distance on the surface one must travel from an initial point for the correlation function to drop to  $1/e$  of its maximum value.  $T_{\text{short}}$  is representative of the rms slopes of the surface facets ( $\sqrt{2} \sigma/T_{\text{short}}$ ).

### 3. THE THEORETICAL AND EXPERIMENTAL RESULTS FOR METALLIC ROUGH SURFACES AT OPTICAL FREQUENCIES

In this section, an attempt will be made to compare the one-dimensional, exact triple integral solution to some of the data taken at optical frequencies by O'Donnell and Mendez.<sup>1,2</sup> They made a number of measurements of the diffuse power scattered from rough metallic surfaces at optical frequencies for various angles of incidence.

Note, after the figures in Sections 3 and 4 were completed, we discovered an error in the factor outside the integral. It should be  $k/(4\pi^2)$  rather than the original  $\pi k$ . The shapes of the calculated curves do not change, but the magnitudes should be shifted by a factor of  $1/(4\pi^2)$  or -20.9 dB.

In the experiments of Mendez and O'Donnell,<sup>1</sup> they scattered a laser beam ( $\lambda = 0.633 \mu\text{m}$ ) from a rough aluminum surface. They determined the standard deviation in surface height  $\sigma$  to be 1.0 to 2.0  $\mu\text{m}$ , and the surface correlation function to be Gaussian with a  $1/e$  width  $T = 1.8 \mu\text{m}$ . They observed that there is no backscatter enhancement in the antispecular ( $\theta_s = -\theta_i$ ) direction, when  $\theta_i = 20^\circ$ . They state that the enhanced backscattering can be easily seen for angles of incidence  $\theta_i \geq 60^\circ$ .

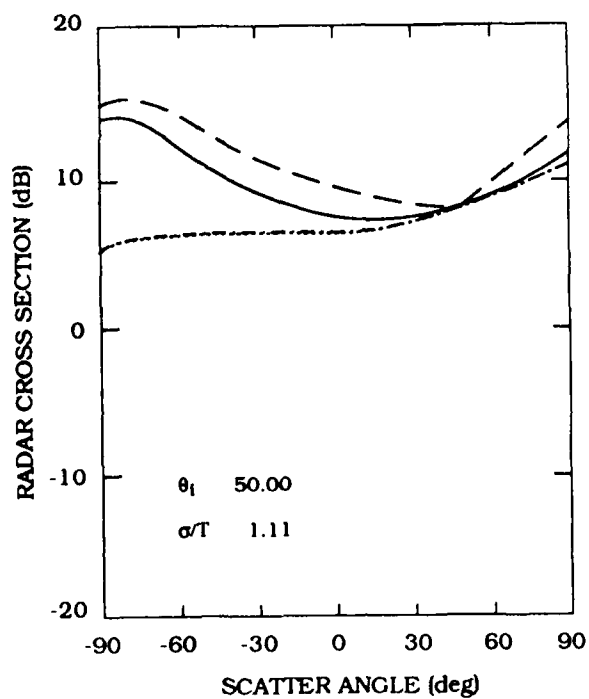
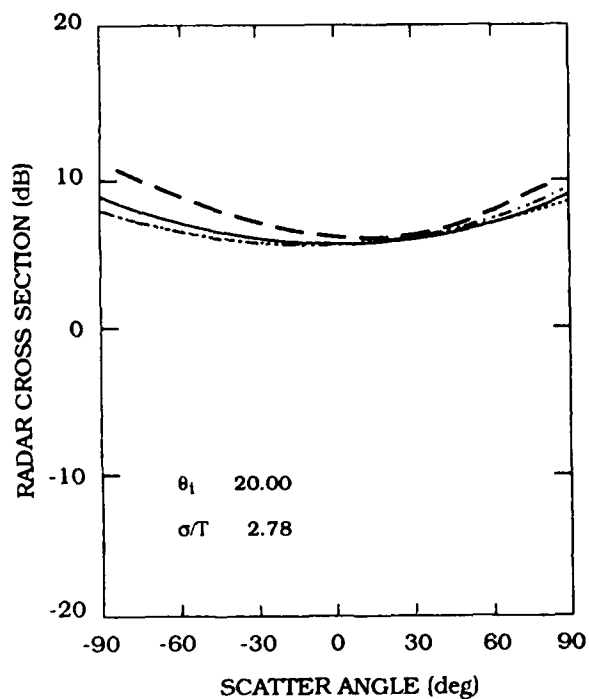
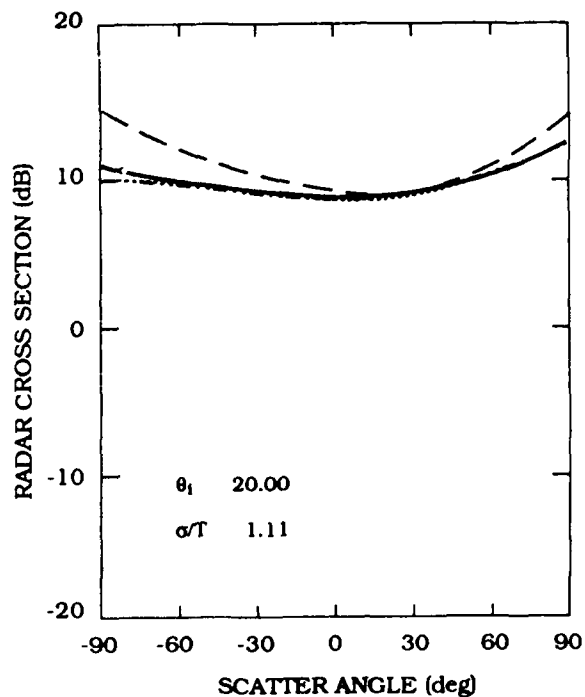
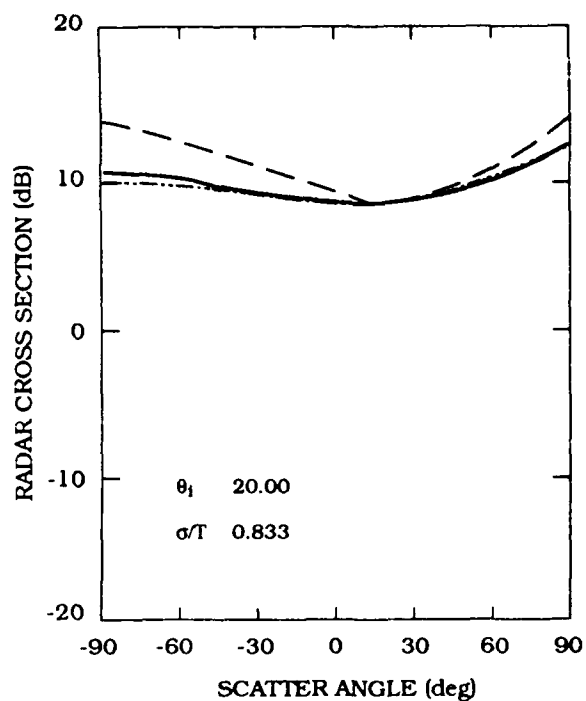
In Figure 1, the one-dimensional PO models presented in Section 2 ( $\sigma^\circ$  models) are plotted vs the scattering angle  $\theta_s$  for an aluminum surface with  $\epsilon = -25.3 + j 15.1$ . This value of the complex dielectric constant for metals at optical frequencies is based upon the free electron model (see Born and Wolf)<sup>16</sup> of a metal. The surface correlation length is taken to be  $T = 1.8 \mu\text{m}$ . In the first sub-figure of Figure 1,  $\theta_i = 20^\circ$ ,  $\sigma = 1.5 \mu\text{m}$ , and there is no backscatter enhancement. This is in agreement with Mendez and O'Donnell's data. In the second sub-figure of Figure 1,  $\theta_i = 20^\circ$ ,  $\sigma = 2 \mu\text{m}$ , and the exact PO triple integral solution shows no backscatter enhancement. In the third sub-figure of Figure 1,  $\theta_i = 20^\circ$  and the rms surface slopes have been greatly increased so  $\sigma/T = 2.78$ ; however, there is a slight backscatter enhancement at  $\theta_s = -90^\circ$ . In the fourth sub-figure of Figure 1,  $\theta_i$  has been increased to  $50^\circ$  and  $\sigma/T = 1.11$ . It may be readily observed that there is backscatter enhancement at  $\theta_s = -90^\circ$ . This also is in agreement with Mendez and O'Donnell's data. It should be noted that the PO,  $F(\mu_{\text{sp}})$  approximation and the GO approximation also predict backscatter enhancement in the third and fourth sub-figures of Figure 1, but these results are not reliable; both approximations are beyond their range of validity since they were derived under the assumptions of small rms surface slopes, ( $\sigma/T < 1$ ).

<sup>16</sup> Born, M. and Wolf, E. (1959) *Principles of Optics*, Pergamon Press.

Note, quite often these two approximations predict the same RCS  $\sigma^0$  values, hence the lines are plotted on top of one another, giving the appearance of a long dashed line.

In Figure 2, the angle of incidence  $\theta_i$  is equal to  $70^\circ$  and  $\sigma$  is  $1 \mu\text{m}$  with  $T = 1.8 \mu\text{m}$  for a rough aluminum surface irradiated with laser light ( $\lambda = 0.633 \mu\text{m}$ ). These are the parameters given by Mendez and O'Donnell.<sup>1</sup> It may be readily discerned that the triple integral solution predicts enhanced backscatter, and also by the PO,  $F(\mu_{sp})$  model and the GO model. For  $\theta_i = 70^\circ$ , Mendez and O'Donnell reported observation of enhanced backscatter for aluminum.





$\lambda$  0.630E-06     $T$  0.180E-05     $\epsilon$  (-25.3, 15.1)  
 — TRIPLE INT,    - - - PO, F INT,    - - - PO, F( $\mu_{sp}$ ),    ..... PO, F(0),    - - - GO, F( $\mu_{sp}$ )

Figure 1. The Normalized Cross Section  $\sigma^\circ$  vs Scattering Angle for an Aluminum Surface with Different Roughness Conditions.

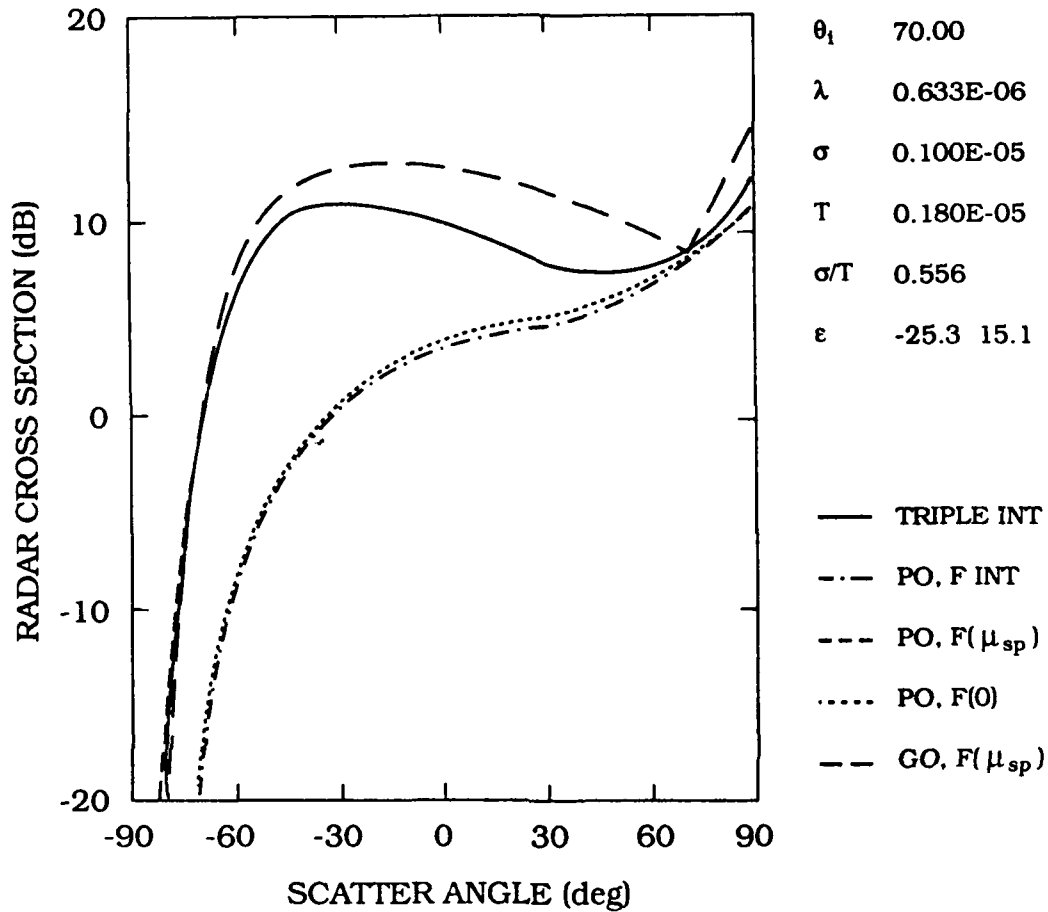


Figure 2. The Normalized Cross Section  $\sigma^0$  vs Scattering Angle for an Aluminum Surface,  $\theta_i = 70^\circ$ ,  $\sigma/T = 0.556$ .

In Figure 3, all the parameters are the same as in Figure 2, except that the upper limit for  $\sigma$  reported by Mendez and O'Donnell is used ( $\sigma = 2 \mu\text{m}$ ). Here, again, for  $\theta_i = 70^\circ$ , the triple integral solution predicts enhanced backscatter, in accord with Mendez and O'Donnell's data. Once again, the PO, F( $\mu_{sp}$ ) model and the GO model predict enhanced backscatter, even though both models are being used beyond their range of validity ( $\sigma/T = 1.11$ ).

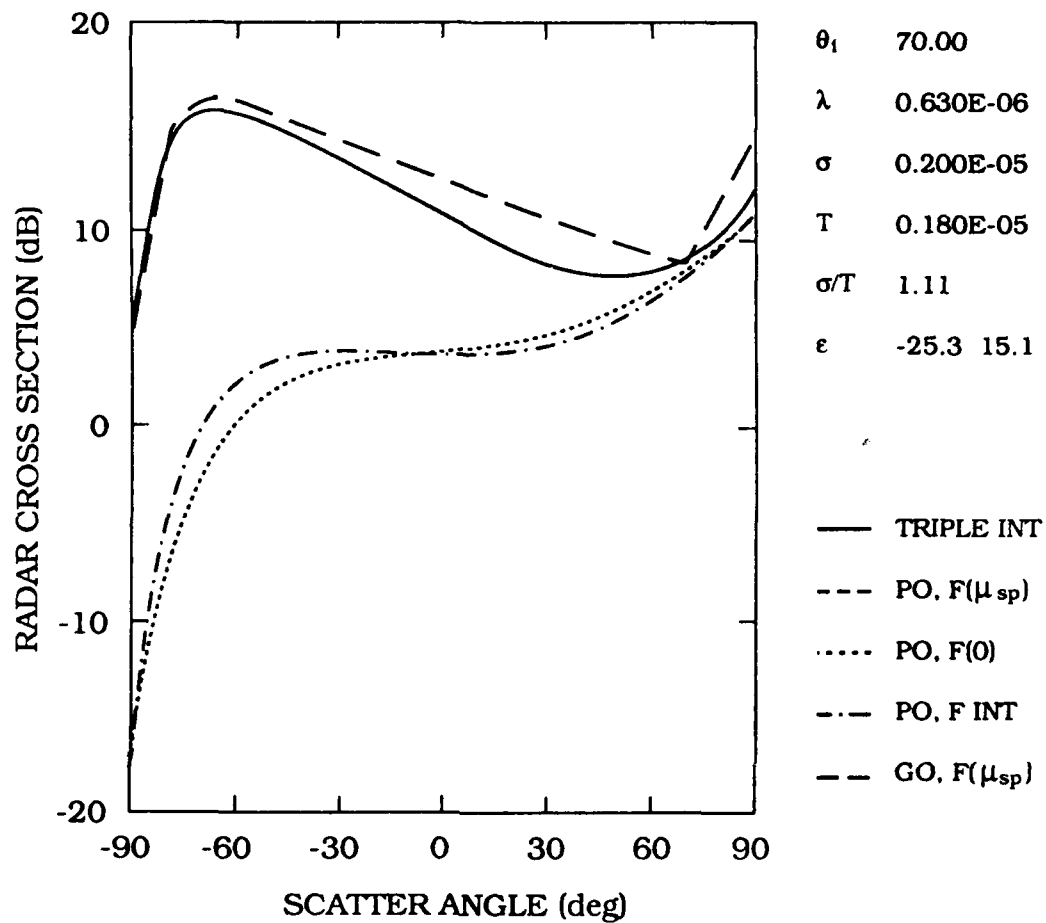


Figure 3. The Normalized Cross Section  $\sigma^o$  vs Scattering Angle for an Aluminum Surface,  $\theta_i = 70^\circ$ ,  $\sigma/T = 1.11$ .

In Figure 4 the parameters are the same as in Figure 3, except that the angle of incidence  $\theta_i = 60^\circ$ . Here, also, there is enhanced backscatter, although it is not as pronounced as in Figure 3 ( $\theta_i = 70^\circ$ ). This trend is in agreement with the experimental data.

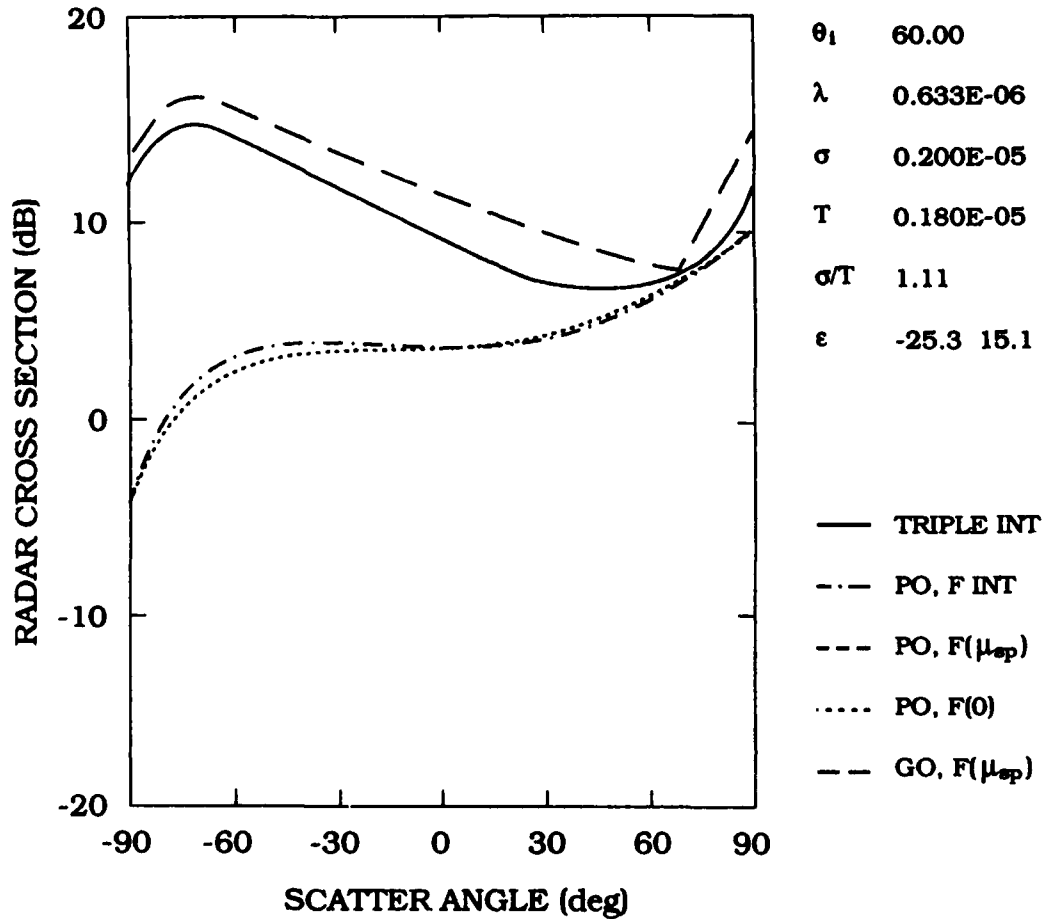


Figure 4. The Normalized Cross Section  $\sigma^\circ$  vs Scattering Angle for an Aluminum Surface,  $\theta_i = 60^\circ$ ,  $\sigma/T = 1.11$ .

In Figure 5,  $\theta_i = 70^\circ$  and the correlation length for a rough aluminum surface has been increased to  $T = 4.5 \mu\text{m}$ . Again, it may be readily discerned that there is enhanced backscatter. This is also true in Figure 6, where  $\theta_i = 70^\circ$ ,  $T = 1.8 \mu\text{m}$  and the standard deviation in surface height has been decreased to  $\sigma = 0.9 \mu\text{m}$ . Figure 7 shows the normalized received power scattered from a gold coated diffuser at  $\lambda = 0.6333 \mu\text{m}$  with a vertically polarized incident wave. The normalized intensity (in dB) is plotted vs the scattering angle for  $\phi = 0^\circ$  (in the plane of incidence). O'Donnell and Mendez<sup>2</sup> formed a histogram (Gaussian) of the surface height data measured with a profilometer; the standard deviation in height was  $\sigma = 2.27 \mu\text{m}$ . The surface correlation function was also measured and found to be Gaussian with a correlation length  $T = 20.9 \mu\text{m}$ . The free electron theory of metals irradiated at optical frequencies<sup>16</sup> gives the following value for the complex dielectric constant for gold:

$\epsilon = -7.8 + j 2.7$ . It may be discerned from Figure 7 that O'Donnell and Mendez's<sup>2</sup> experimental data clearly shows enhanced backscatter in the antisp specular direction,  $\theta_s = -70^\circ$ . In Figure 8, the  $\sigma^\circ$  values are plotted vs  $\theta_s$  for the triple integral solution and the various approximations for the conditions of O'Donnell and Mendez's<sup>2</sup> gold diffuser experiment. It is readily observed that none of the theoretical models predict enhanced backscatter. This is because all these models are single scattering theories, and provide no physical mechanism for enhanced backscatter at such low rms surface slopes ( $\sigma/T = 0.1$ ). When the rms surface slopes are intermediate or large ( $\sigma/T \geq 1$ ), then there are enough facets oriented so that specular scattering from these facets can reach a maximum in the backward direction. In this case, the single scatter physical optics model can show backscatter enhancement.

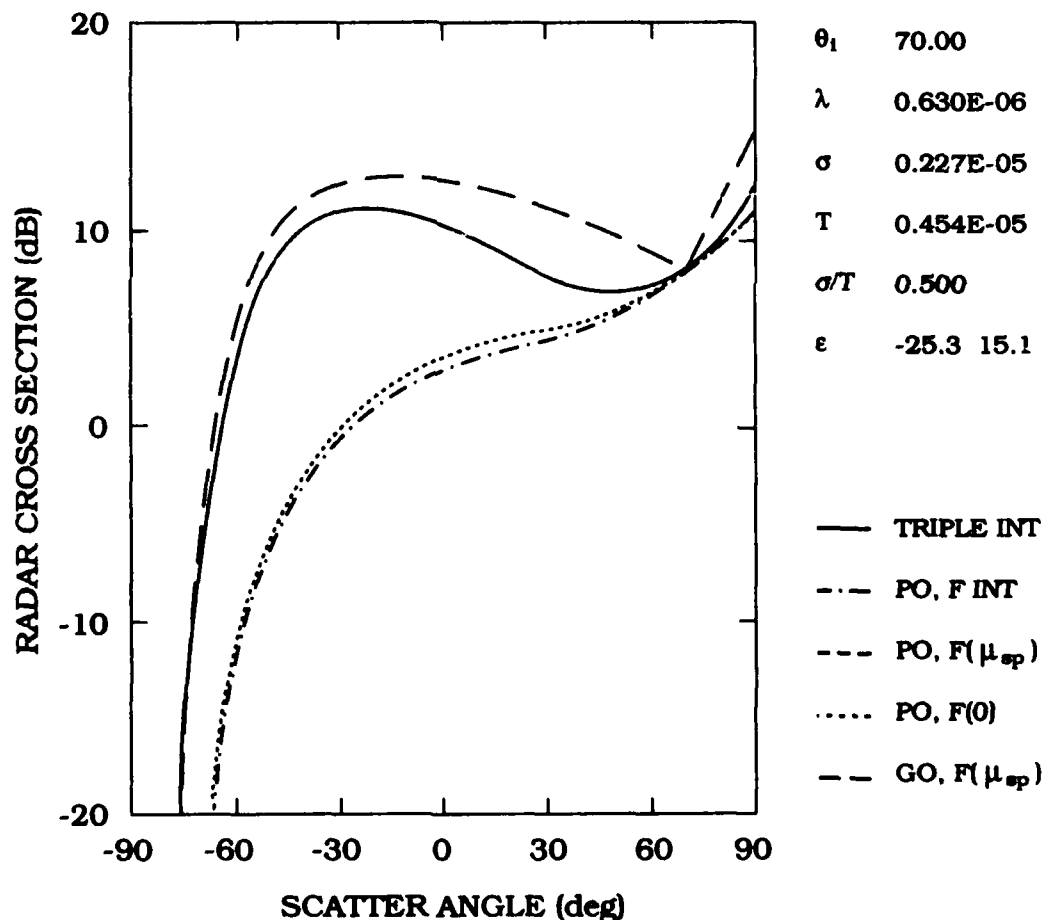


Figure 5. The Normalized Cross Section  $\sigma^\circ$  vs Scattering Angle for an Aluminum Surface,  $\theta_i = 70^\circ$ ,  $\sigma/T = 0.5$ .

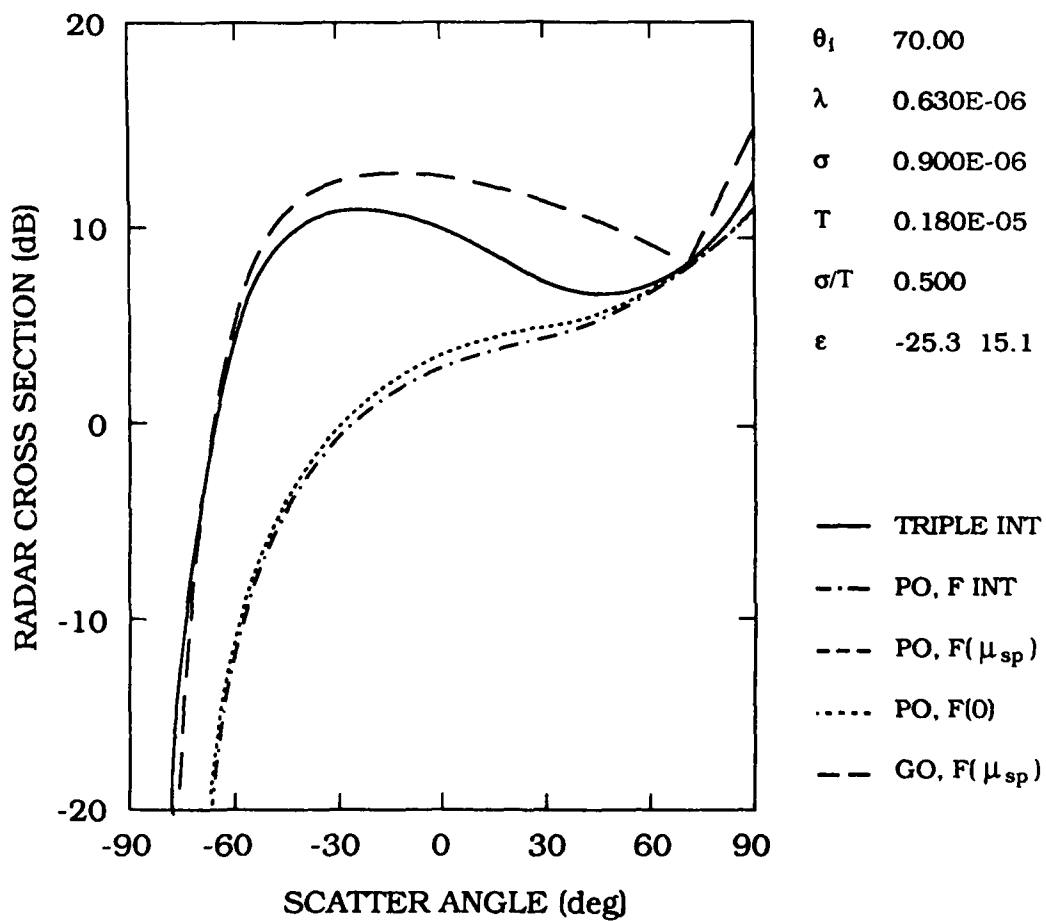


Figure 6. The Normalized Cross Section  $\sigma^0$  vs Scattering Angle for an Aluminum Surface,  $\theta_i = 70^\circ$ ,  $\sigma/T = 0.5$  with Large Standard Deviation in Surface Height.

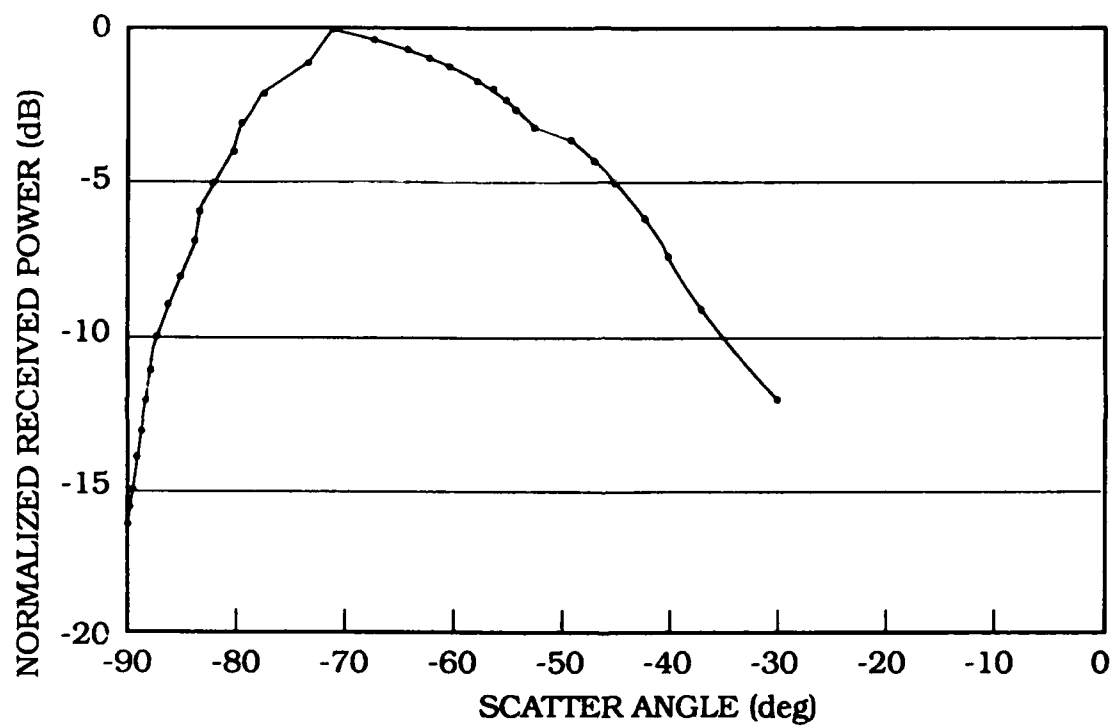


Figure 7. The Normalized Intensity vs Scattering Angle for a Gold Diffuser, Experimental Data

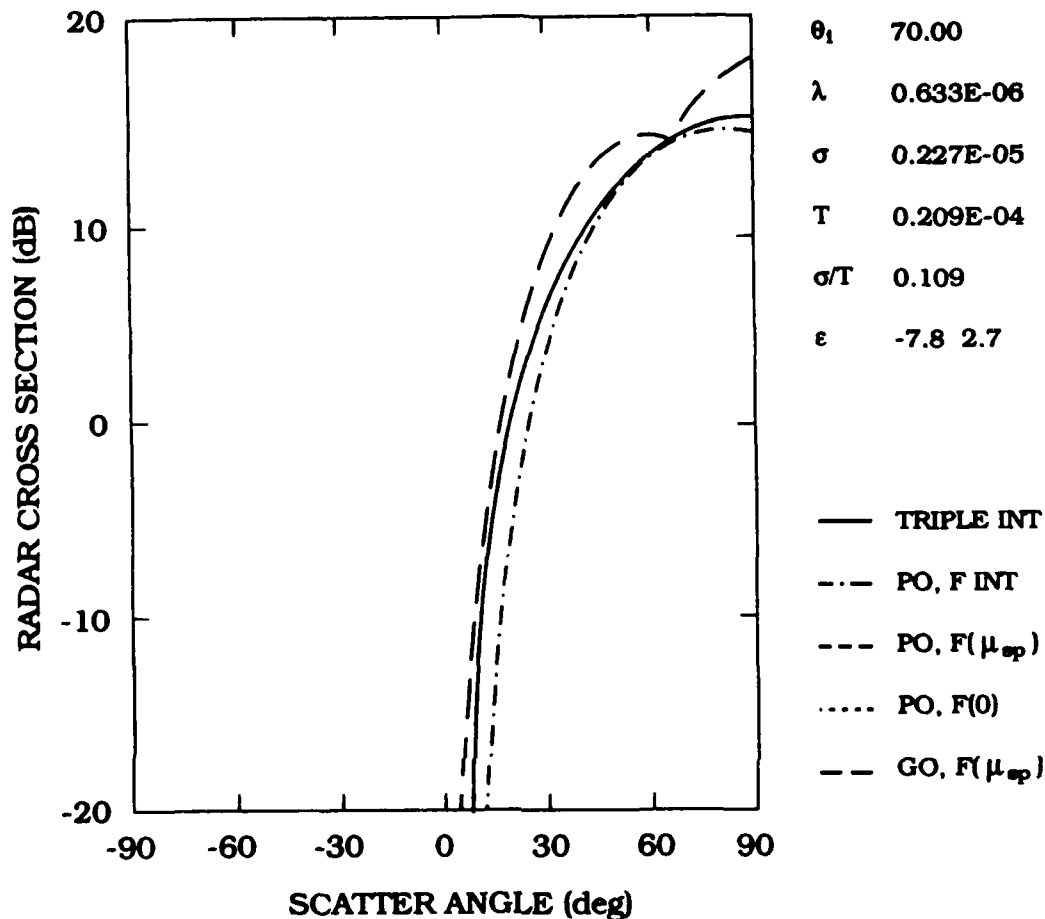


Figure 8. The Normalized Cross Section  $\sigma^0$  vs Scattering Angle for a Gold Surface,  $\theta_1 = 70^\circ$ ,  $\sigma/T = 0.109$ .

In Figure 9,  $\epsilon = -7.8 + j 2.7$  for gold,  $\theta_1 = 70^\circ$  and the rms slope is increased from  $\sigma/T = 0.109$  to 0.216 by decreasing the correlation length,  $T = 10.5 \mu\text{m}$ . Here, the rms surface slopes are still too small to produce any enhanced backscatter. In Figure 10, the parameters are the same as in Figure 9, except for the correlation length, which has been further reduced to  $T = 5.25 \mu\text{m}$ . Now,  $\sigma/T = 0.432$  is sufficiently large so that there is a small amount of enhanced backscatter. In Figure 11, the parameters are the same as in Figure 10, except for the correlation length, which again has been even further reduced to  $T = 2.0 \mu\text{m}$ . It may easily be discerned that with  $\sigma/T = 1.135$ , there is considerable backscatter enhancement for this gold diffuser.



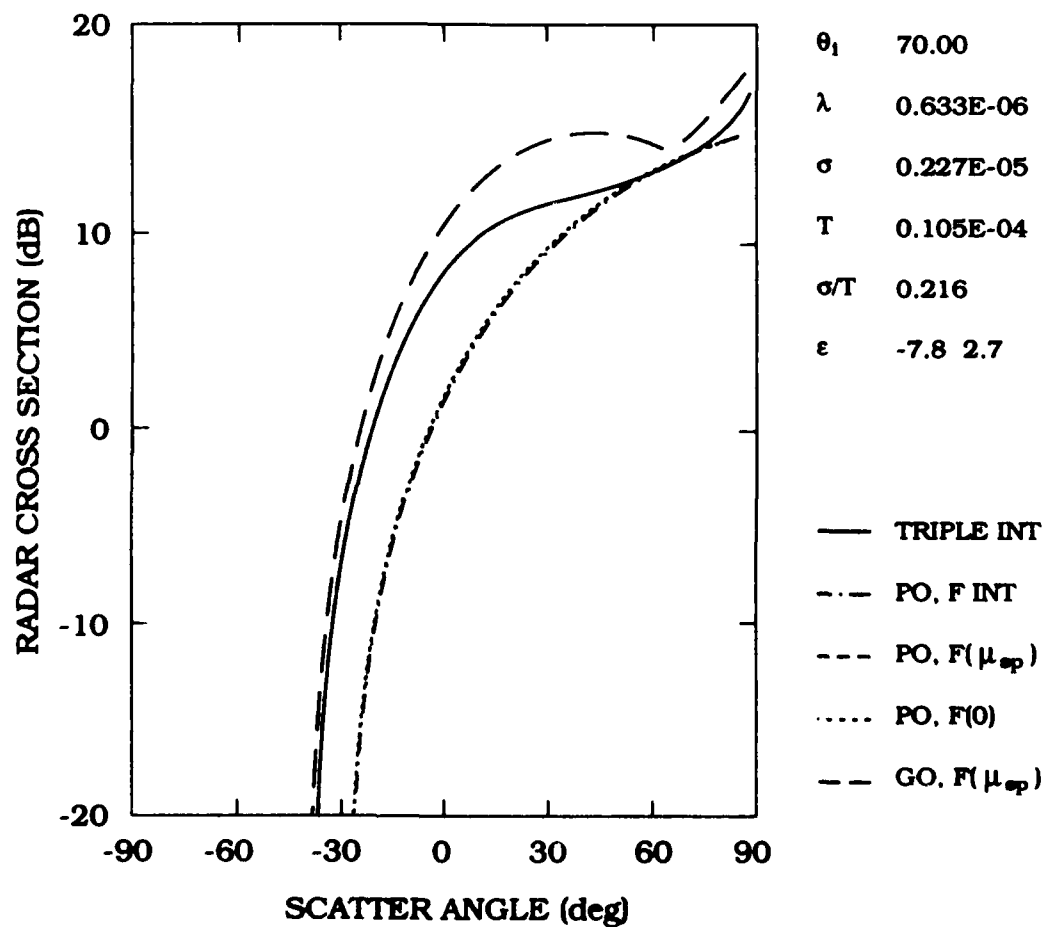


Figure 9. The Normalized Cross Section  $\sigma^\circ$  vs Scattering Angle for a Gold Surface,  $\theta_i = 70^\circ$ ,  $\sigma/T = 0.216$ .

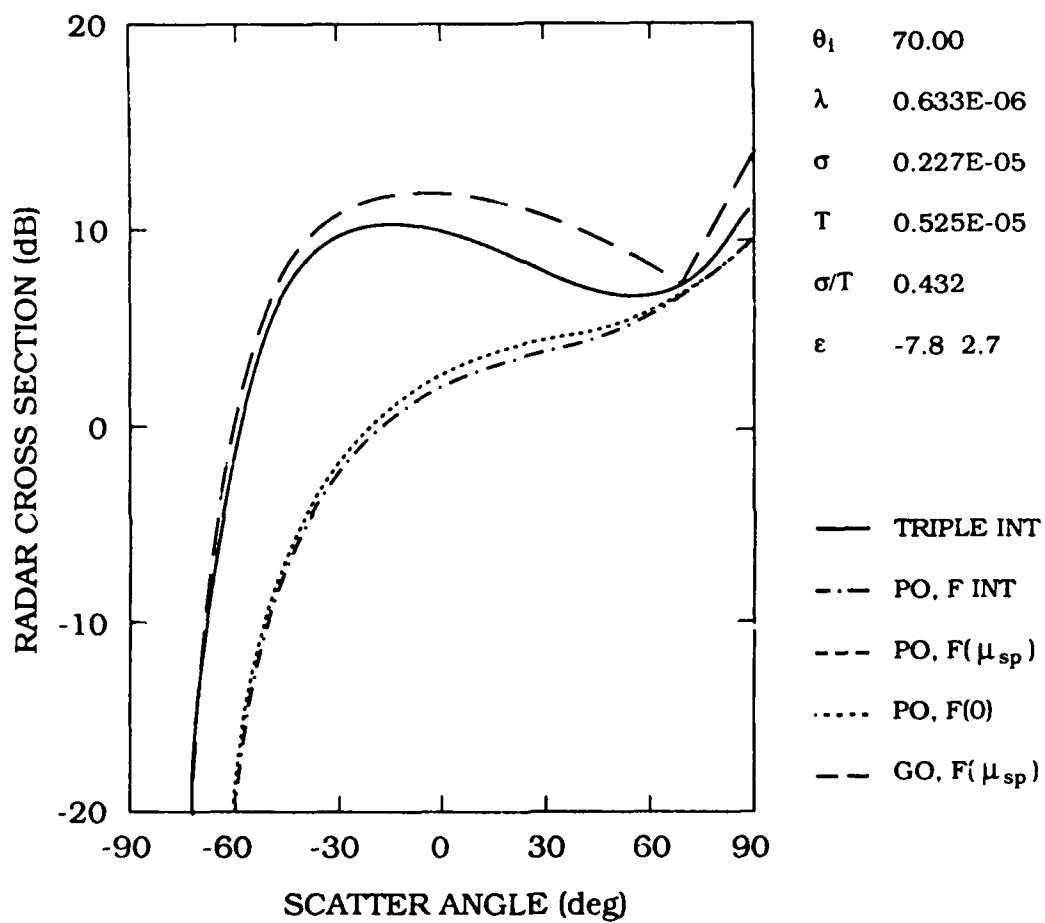


Figure 10. The Normalized Cross Section  $\sigma^o$  vs Scattering Angle for a Gold Surface,  $\theta_i = 70^\circ$ ,  $\sigma/T = 0.432$ .

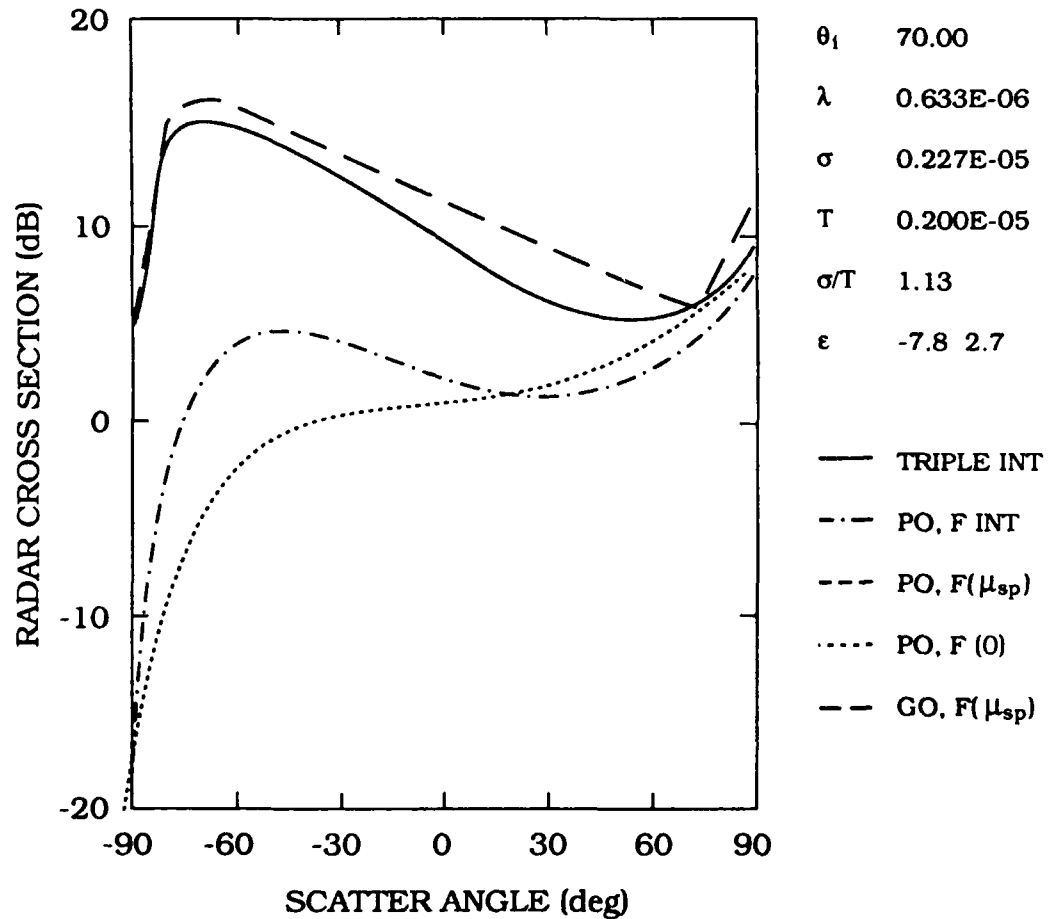


Figure 11. The Normalized Cross Section  $\sigma^0$  vs Scattering Angle for a Gold Surface,  $\theta_i = 70^\circ$ ,  $\sigma/T = 1.135$ .

In Figures 12, 13, and 14, the two correlation lengths surface roughness model discussed in Section 2 is investigated. Here,  $\epsilon = -7.8 + j 2.7$  for a gold plated rough surface and  $\lambda = 0.633 \mu\text{m}$ . The correlation length that governs the decorrelation properties of the scattering facets  $T_{\text{long}} = 20.9 \mu\text{m}$  in these three figures, in accordance with O'Donnell and Mendez's<sup>2</sup> experimental data. The correlation length  $T_{\text{short}}$  that governs the rms surface slopes in Figure 12 is chosen so that  $\sigma/T_{\text{short}} = 0.454$ . It may be readily noted that there is no backscatter at all from such a surface, much less backscatter enhancement. In Figure 13,  $T_{\text{short}}$  has been reduced so that  $\sigma/T_{\text{short}} = 1.14$ . However, even with an rms surface slope greater than 1, there is no backscatter enhancement. In Figure 14,  $T_{\text{short}}$  has been further reduced so that now  $\sigma/T_{\text{short}} = 2.27$ . Here, one may observe that there is some backscatter, but not enough to be considered an enhancement in the backscatter direction.

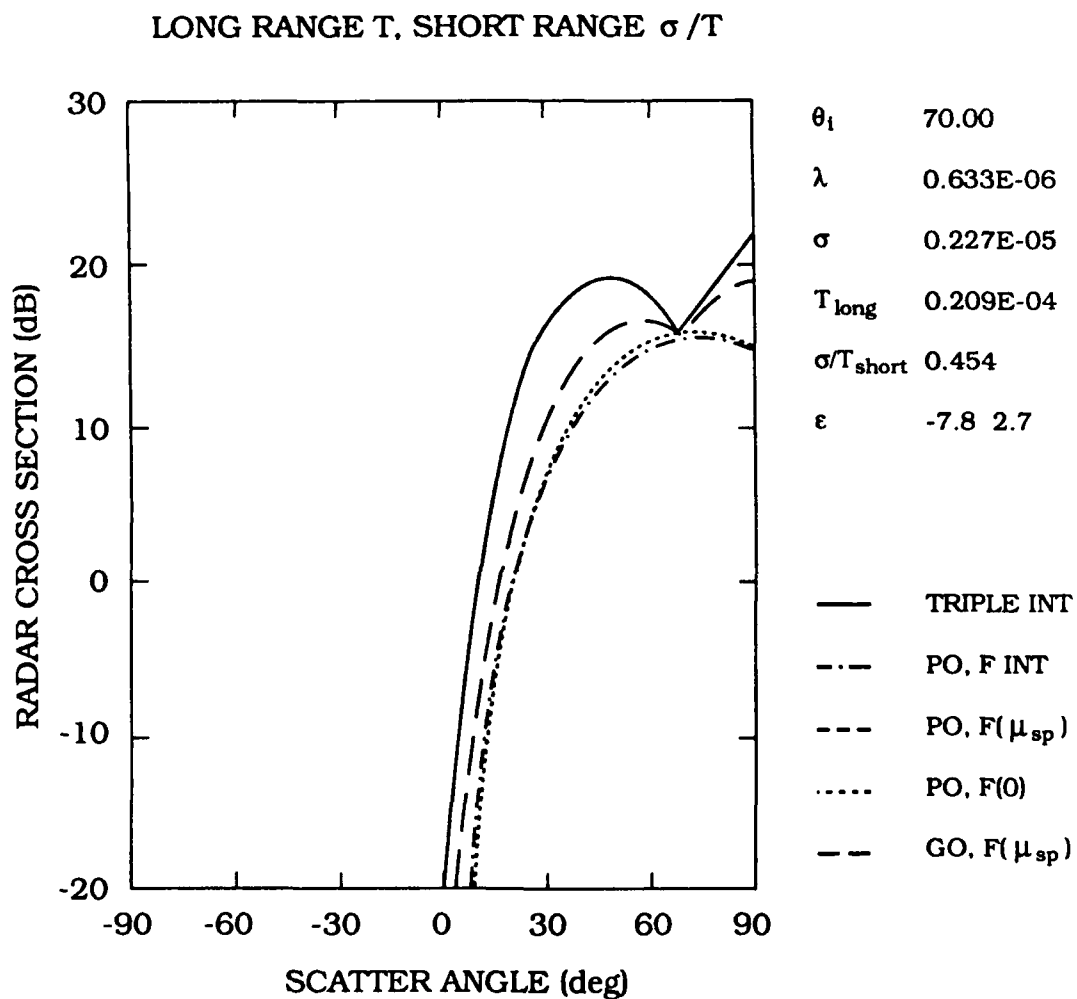


Figure 12. The Normalized Cross Section  $\sigma^\circ$  vs Scattering Angle for a Gold Surface,  $\theta_i = 70^\circ$ , Two Correlation Lengths  $\sigma/T_{\text{short}} = 0.4504$ .

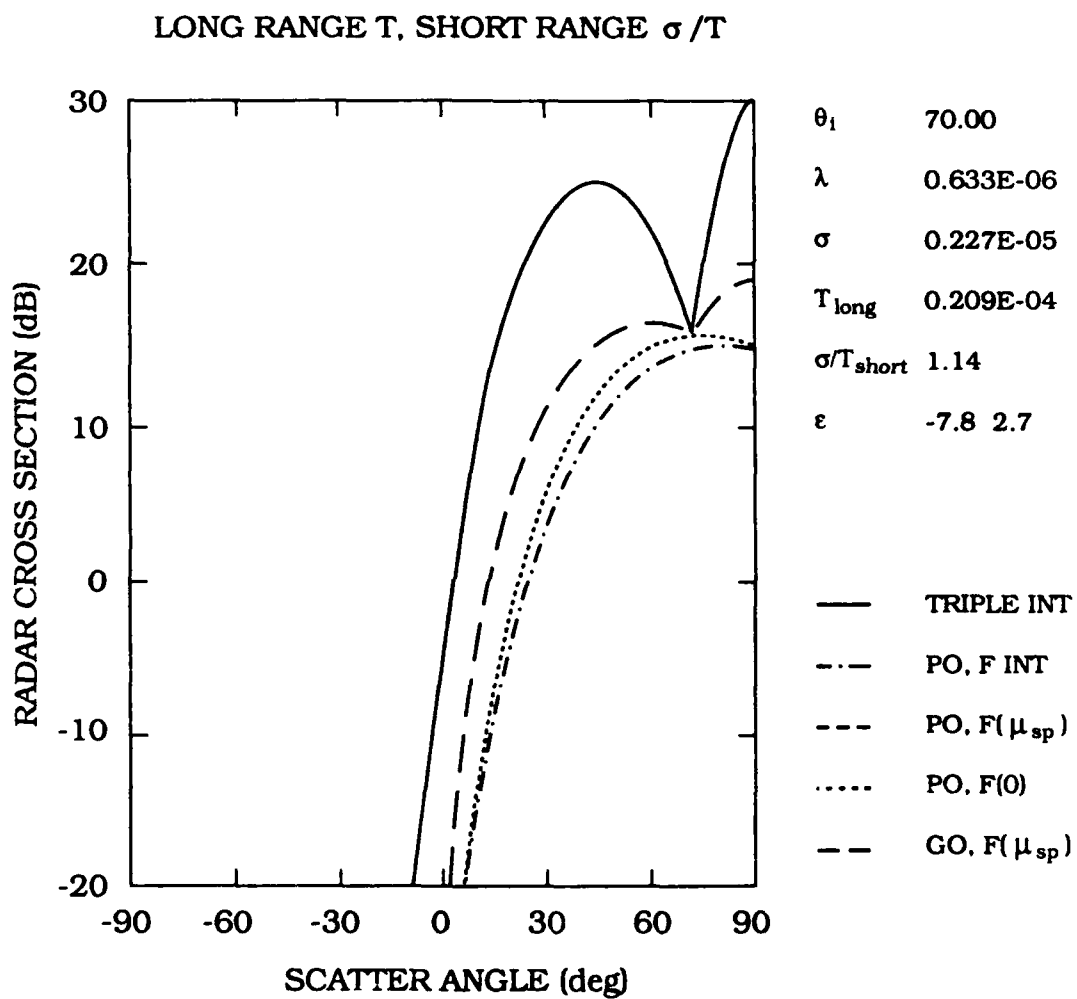


Figure 13. The Normalized Cross Section  $\sigma^\circ$  vs Scattering Angle for a Gold Surface,  $\theta_i = 70^\circ$ , Two Correlation Lengths  $\sigma/T_{\text{short}} = 1.14$ .

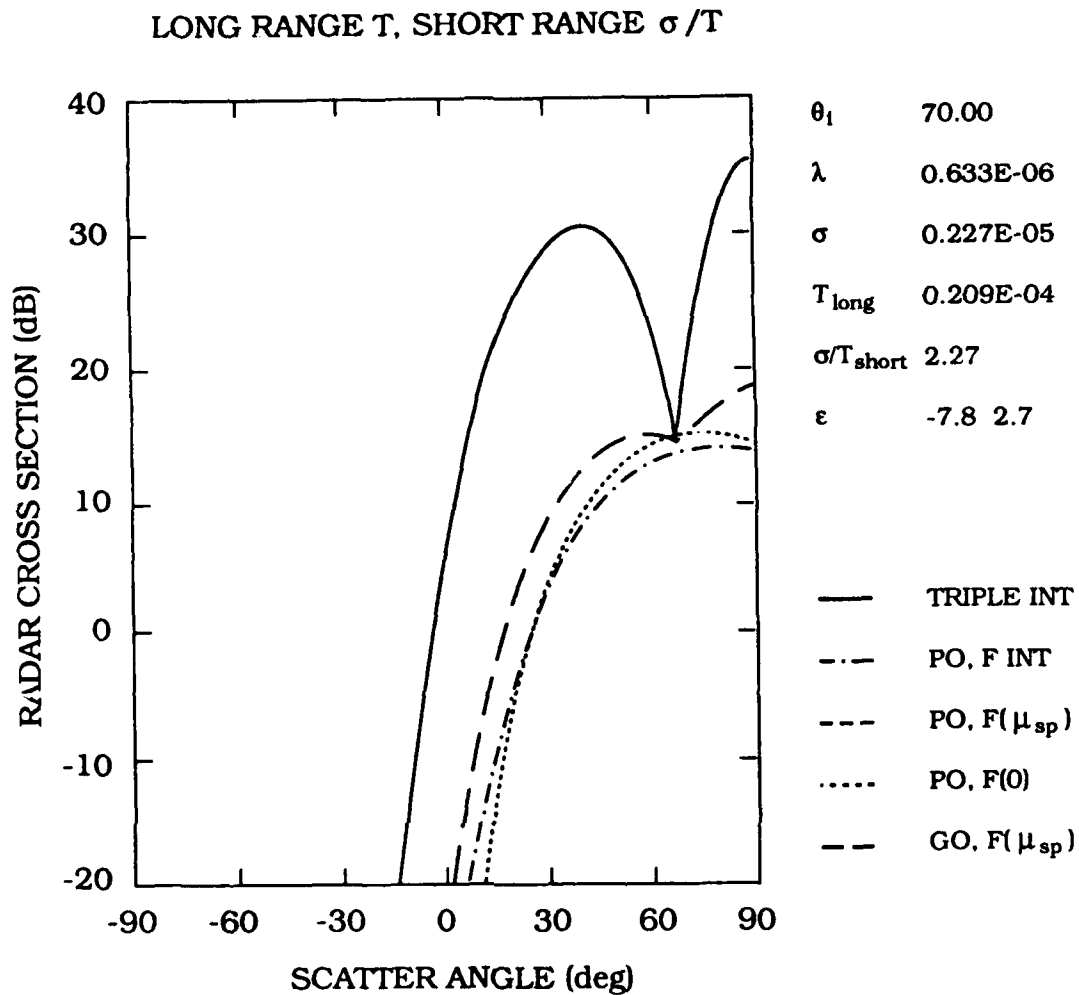


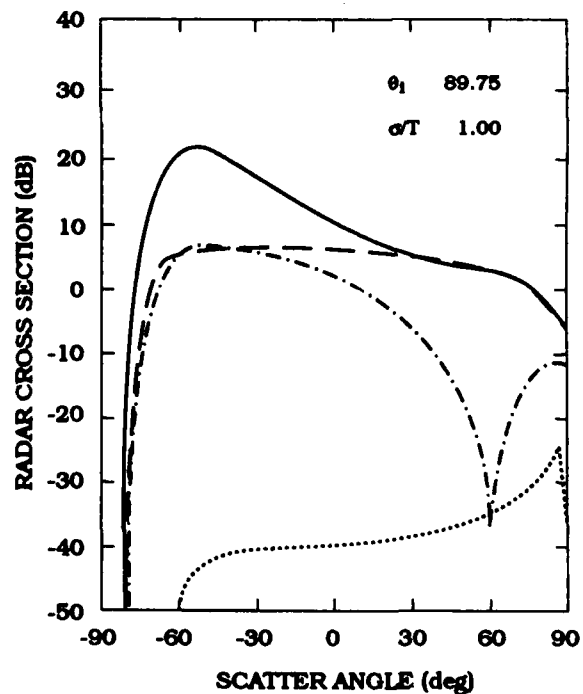
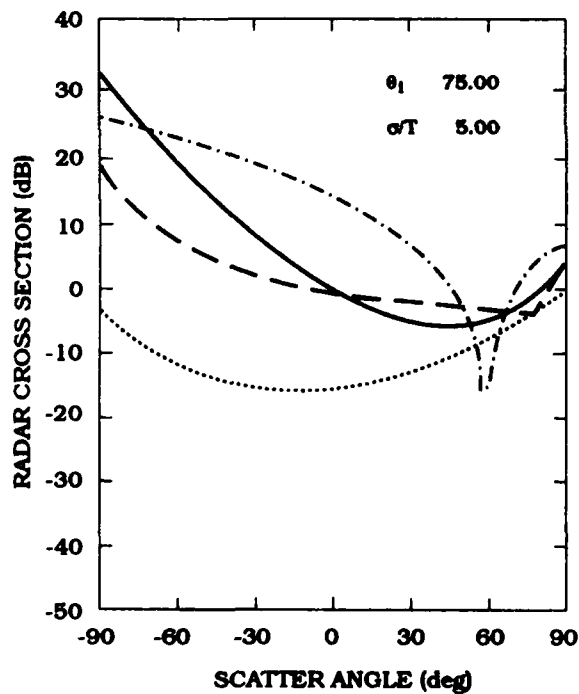
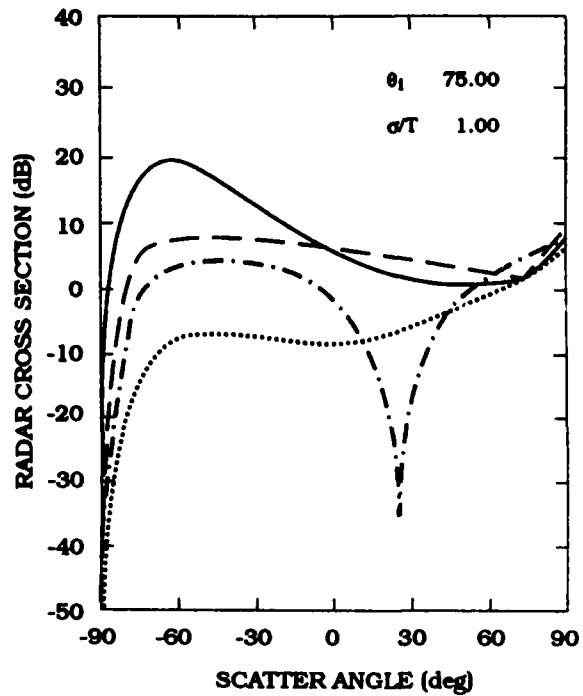
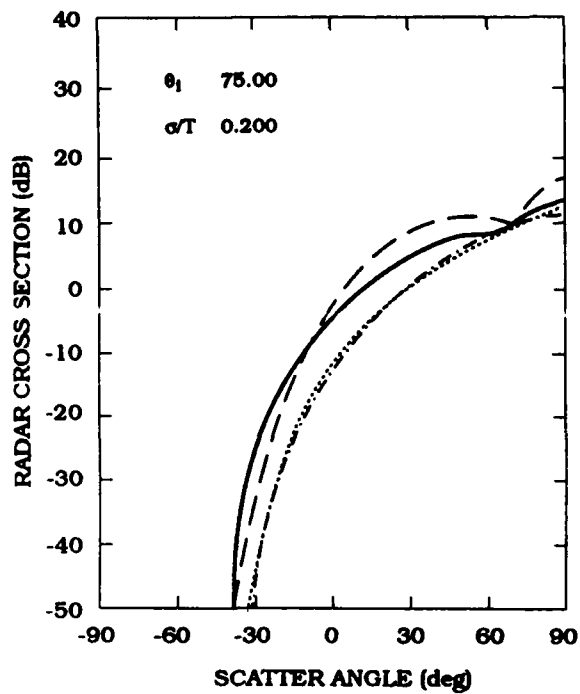
Figure 14. The Normalized Cross Section  $\sigma^\circ$  vs Scattering Angle for a Gold Surface.  $\theta_i = 70^\circ$ . Two Correlation Lengths  $\sigma/T_{\text{short}} = 2.27$ .

#### 4. THE THEORETICAL RESULTS FOR DIELECTRIC ROUGH SURFACES AT RADIO FREQUENCIES

For metallic rough surfaces, the theoretical model for  $\sigma^\circ$  predicts backscatter enhancement for moderate to large rms surface slopes, in agreement with some experimental data. This would suggest that backscatter enhancement might occur for dielectric rough surfaces also. In this section, the normalized scattering cross section  $\sigma^\circ$  will be studied for rough dielectric surfaces as a function of elevation scattering angle  $\theta_s$  for various rms surface slopes  $\sqrt{2} \sigma/T$  and angles of incidence  $\theta_i$ . Comparisons will be made between the exact PO, triple integral solution and various approximations; the PO, F INT, F( $\mu_{sp}$ ), F(0) and the high frequency GO

model. Also, it will be shown that for moderate to high rms surface slopes ( $\sigma/T \geq 1$ ), there is backscatter enhancement near the antispecular direction  $\theta_s = -\theta_i$ .

In Figure 15,  $\sigma^0$  is plotted vs elevation scattering angle for a dielectric surface with  $\epsilon = 4.0$ , correlation length  $T = 0.5\text{m}$  and an incident em wavelength of  $0.1\text{m}$ . In the first three sub-figures, the angle of incidence  $\theta_i = 75^\circ$ , and the rms surface slopes successively increase from  $\sigma/T = 0.2$ , to  $1.0$  up to  $5.00$ . It may readily be observed that for small rms slopes, ( $\sigma/T = 0.2$ ), there is no enhanced backscatter. There is good agreement between the exact triple integral solution and the PO,  $F(\mu_{sp})$  model and the GO model. The PO,  $F_{INT}$  model and the PO,  $F(0)$  model show some discrepancy when compared with the exact triple integral solution. In the second sub-figure,  $\sigma/T = 1.0$ , and only the triple integral solution shows enhanced backscatter. The PO,  $F(\mu_{sp})$  model and the GO model show no enhanced backscatter; the PO,  $F_{INT}$  model and the PO,  $F(0)$  model show large discrepancies with the triple integral solution. In the third sub-figure,  $\sigma/T = 5.0$ , and all the approximate models show discrepancies with the exact triple integral solution. The triple integral solution shows enhanced backscatter at  $\theta_s = -90^\circ$ . In the fourth sub-figure of Figure 15, the angle of incidence  $\theta_i = 89.75^\circ$  and  $\sigma/T = 1.0$ . Here again, the triple integral solution shows enhanced backscatter, with all the approximate models exhibiting discrepancies compared with the triple integral solution.



$\lambda$  .100     $T$  0.500     $\epsilon$  4.00

— TRIPLE INT,    - - - - PO, F INT,    - - - - PO, F( $\mu_{ep}$ ),    ..... PO, F(0),    - - - GO, F( $\mu_{ep}$ )

Figure 15. The Normalized Cross Section  $\sigma^0$  vs Scattering Angle for a Dielectric Surface with Different Roughness Conditions.



In Figure 16, the angle of incidence is reduced to  $\theta_i = 60^\circ$  and the dielectric constant  $\epsilon$  remains 4.0. Here, the rms surface slope has an intermediate value  $\sigma/T = 1.0$  and the em wavelength remains at 0.1m. It may readily be discerned that the exact triple integral solution exhibits the most enhanced backscatter and the approximate PO models show discrepancies compared with the triple integral solution.

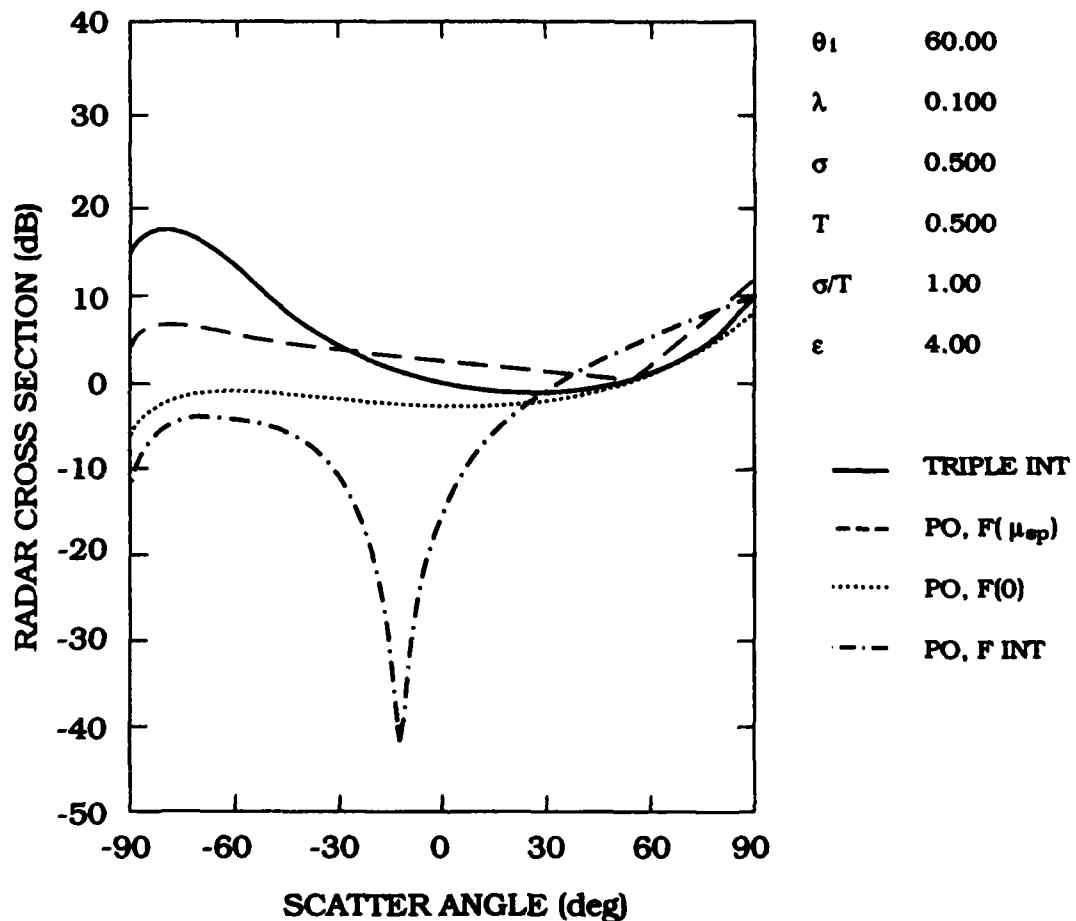


Figure 16. The Normalized Cross Section  $\sigma^\circ$  vs Scattering Angle for a Dielectric Surface,  $\theta_i = 60^\circ$ .

In Figure 17, the normalized cross section  $\sigma^\circ$  of a rough dielectric surface is plotted vs scattering angle  $\theta_s$  for  $\theta_i = 75^\circ$  using a two-dimensional PO scattering model, with a single integral representation for  $\sigma^\circ$  analogous to Eq. (4). It may be noted that there is backscatter enhancement, but it is not nearly as pronounced as the triple integral solution (in the one-dimensional model) shown in the second sub-figure of Figure 1.

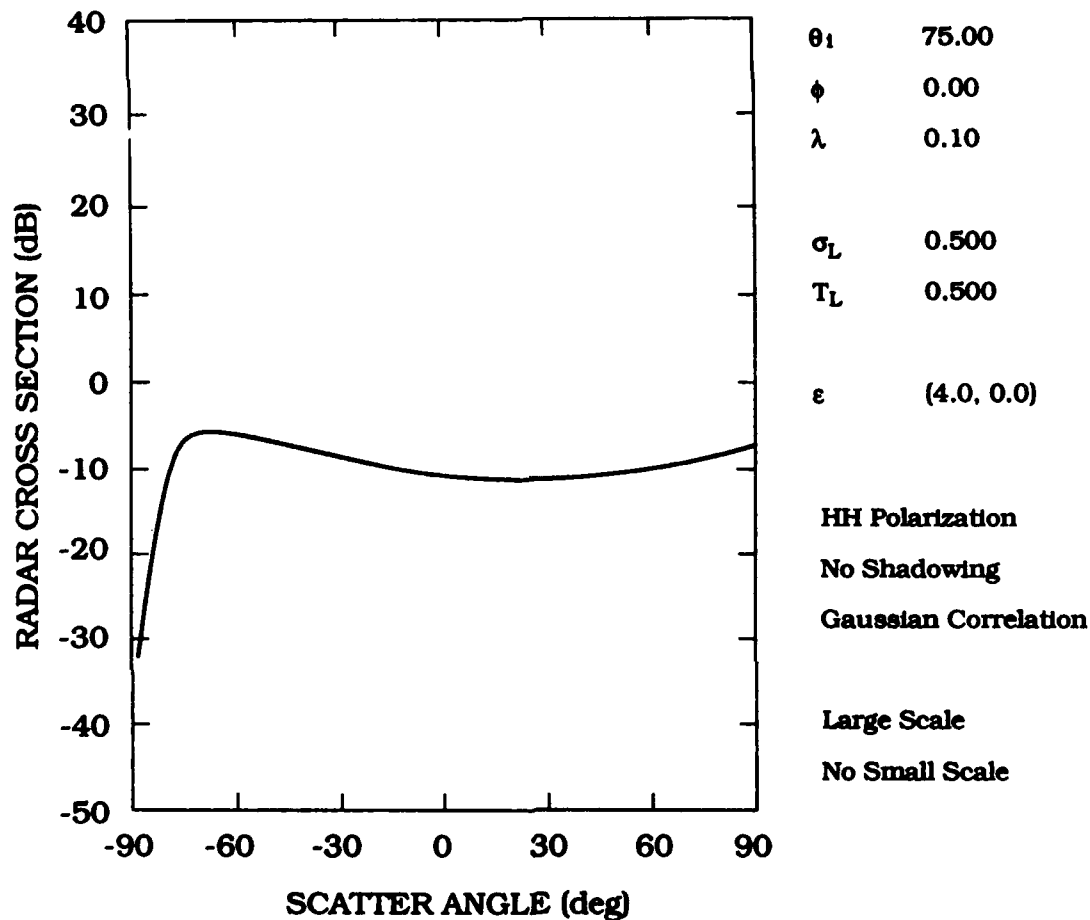


Figure 17. The Normalized Cross Section  $\sigma^0$  vs Scattering Angle for a Dielectric Surface,  $\theta_i = 75^\circ$ .

In Figures 18 through 22, the dielectric constant has been changed to  $\epsilon = 24.0 + j 32$ , which is representative of wet sandy loam. The em wavelength is  $\lambda = 0.03\text{m}$  (X-band). In Figures 18 through 21, the angle of incidence  $\theta_i = 40^\circ$ , and the rms surface slopes became progressively larger. It may be noted from Figures 18 and 19 that there is no backscatter enhancement for  $\sigma/T < 1.0$ . Figures 20 and 21 show that there is backscatter enhancement for  $\sigma/T > 1.0$ , but that it occurs near  $\theta_s \sim -90^\circ$ .

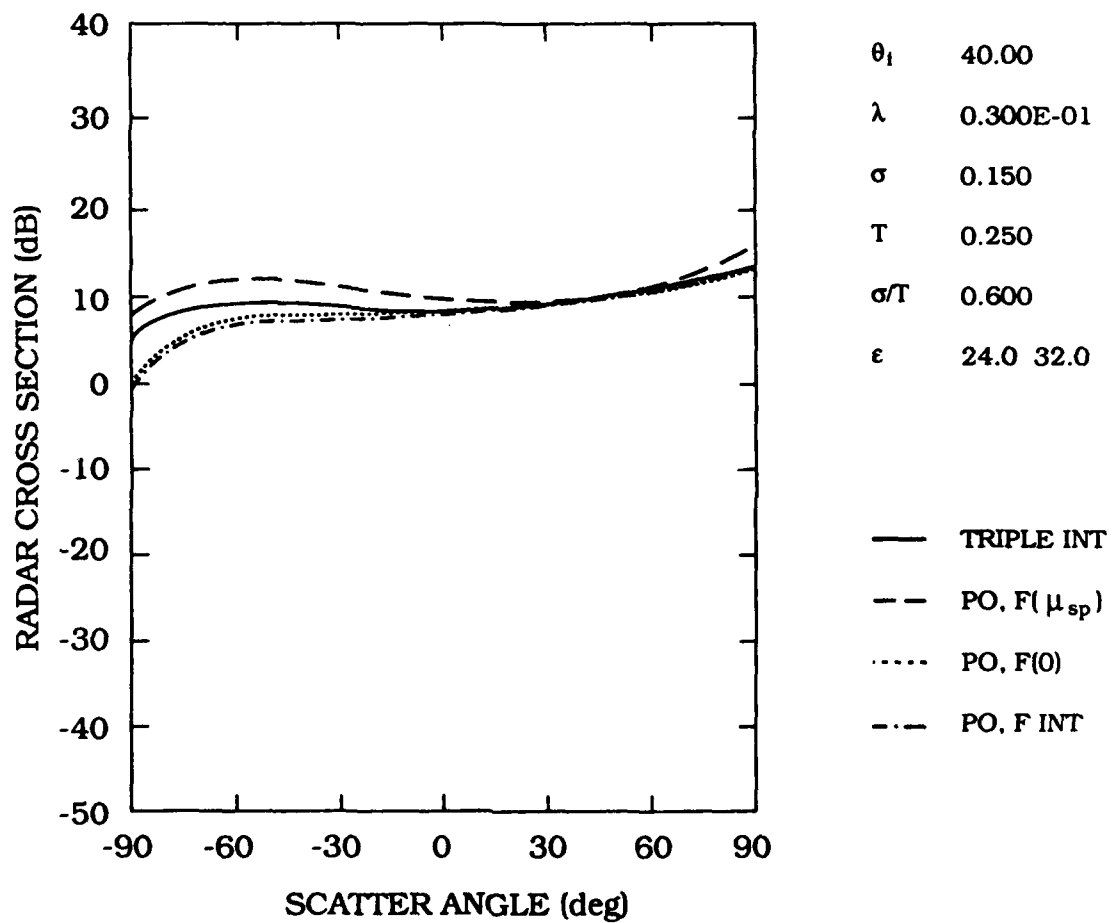


Figure 18. The Normalized Cross Section  $\sigma^o$  vs Scattering Angle for a Lossy Dielectric Surface,  $\theta_i = 40^\circ$ ,  $\sigma/T = 0.6$ .

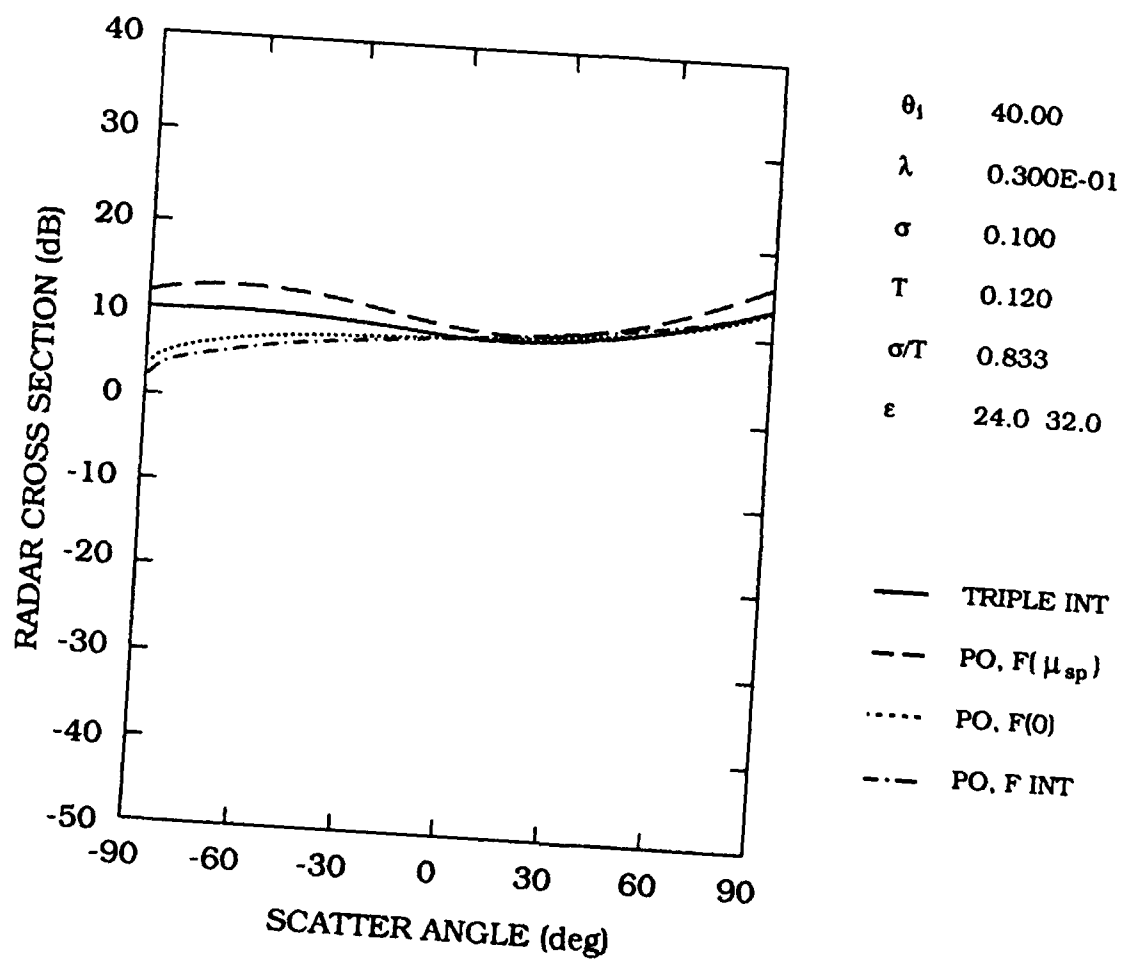


Figure 19. The Normalized Cross Section  $\sigma^o$  vs Scattering Angle for a Lossy Dielectric Surface,  $\theta_i = 40^\circ$ ,  $\sigma/T = 0.833$ .

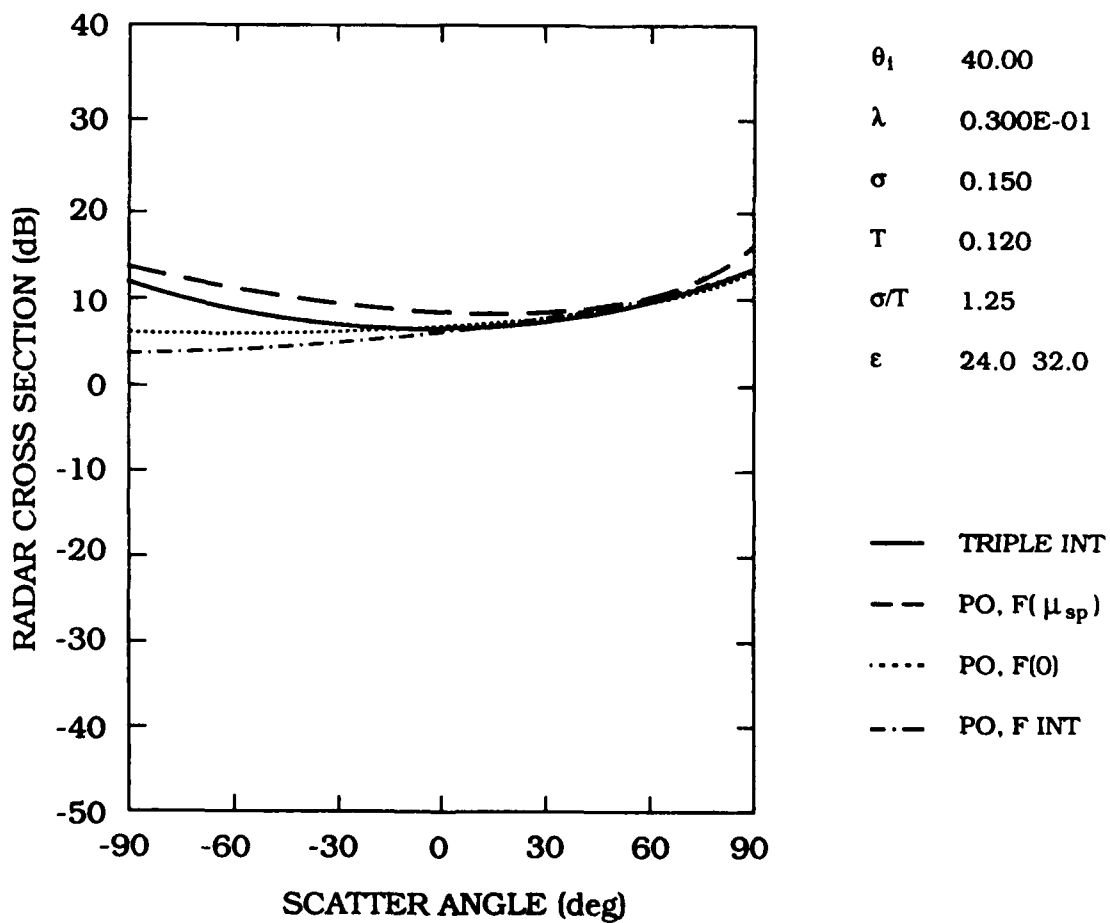


Figure 20. The Normalized Cross Section  $\sigma^\circ$  vs Scattering Angle for a Lossy Dielectric Surface,  $\theta_i = 40^\circ$ ,  $\sigma/T = 1.25$ .

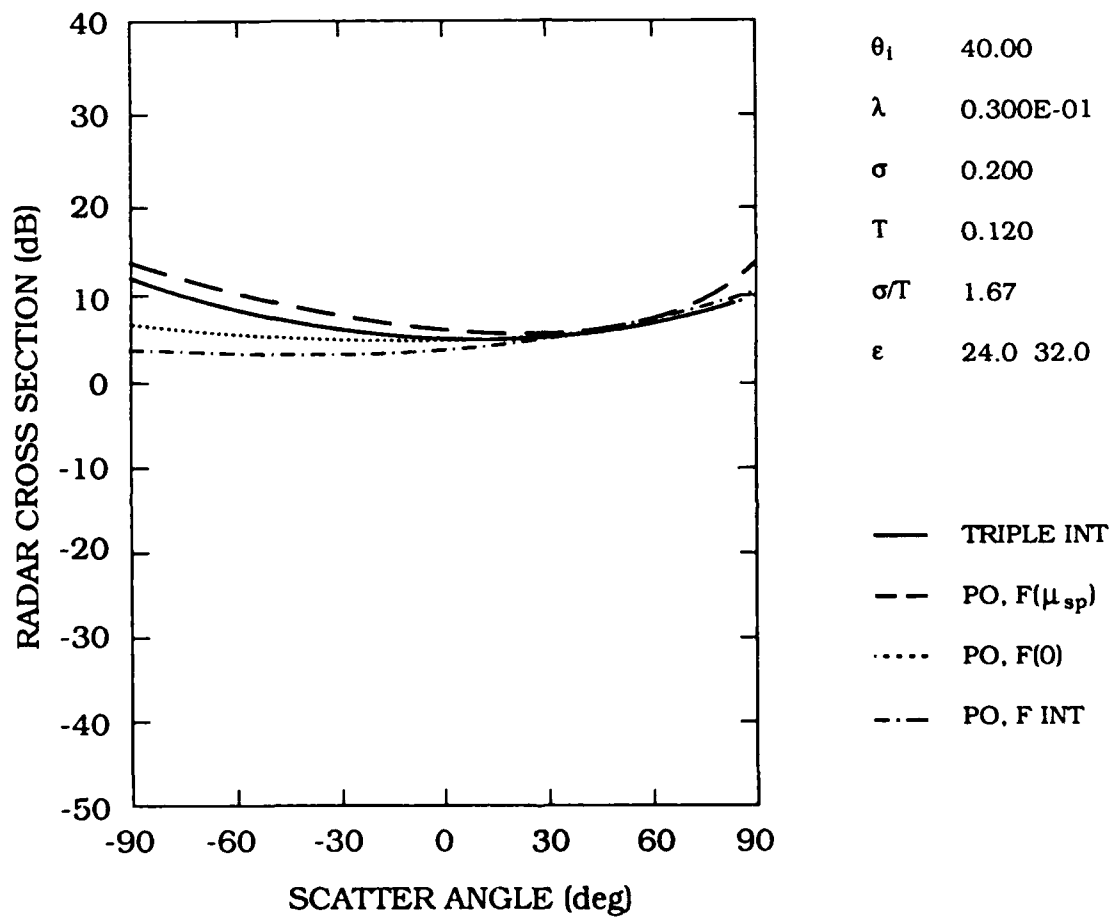


Figure 21. The Normalized Cross Section  $\sigma^o$  vs Scattering Angle for a Lossy Dielectric Surface,  $\theta_i = 40^\circ$ ,  $\sigma/T = 1.67$ .

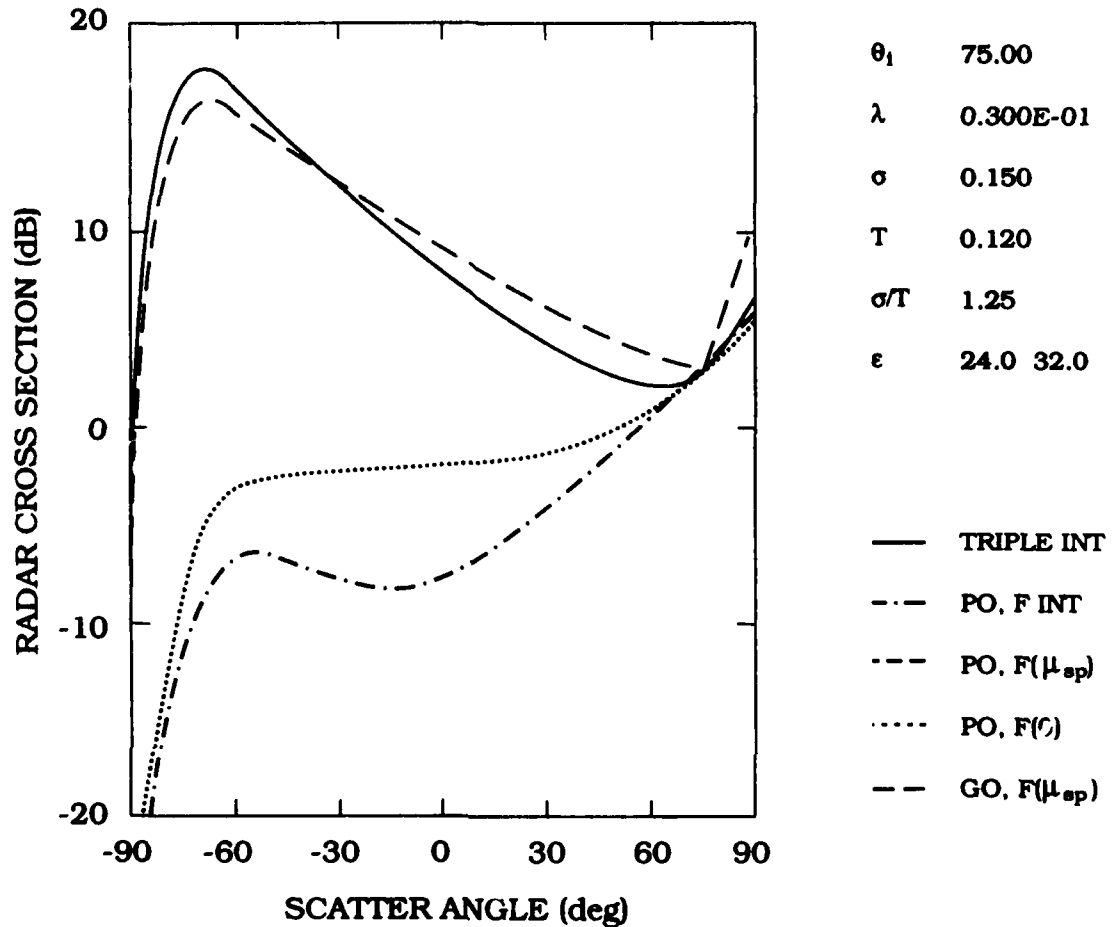


Figure 22. The Normalized Cross Section  $\sigma^0$  vs Scattering Angle for a Lossy Dielectric Surface,  $\theta_i = 75^\circ$ ,  $\sigma/T = 1.25$ .

In Figure 22, the angle of incidence has been increased to  $\theta_i = 75^\circ$  for the dielectric of  $\epsilon = 24 + j 32$ . With a moderate rms slope ( $\sigma/T = 1.25$ ), it may be noted that the triple integral solution and the PO,  $F(\mu_{sp})$  approximation and the GO model all show very large enhanced backscatter. This is analogous to the behavior for metallic surfaces, which is to be expected since a large imaginary part of the complex dielectric constant causes the dielectric to behave more like a metallic material. The two PO approximations,  $F(0)$  and  $F INT$  show very poor agreement with the TI solution. It is to be expected that the PO,  $F(0)$  approximation shows very poor agreement with the exact triple integral solution when  $\sigma/T > 1$ , since it was derived under assumptions that are more restrictive than the  $F(\mu_{sp})$  and GO models; the rms surface slopes are not just small,  $\sigma/T$  must be approximately zero ( $\sigma/T = 0$ ).

## 5. SUMMARY AND CONCLUSIONS

In this report, it has been demonstrated that backscatter enhancement can occur for both rough dielectric surfaces at microwave frequencies and metallic rough surfaces at optical frequencies. This is observed only when the angle of incidence is greater than or equal to  $50^\circ$  and the rms slope of the surface irregularities is equal to or greater than 1.0. The backscatter enhancement is predicted from a physical optics (PO) model that is based on a rough surface scattering formalism in which it is assumed that the surface height  $z$  varies only in one transverse dimension  $x$ . The relatively large rms surface heights imply that the multivariate distribution function describing the statistics of the surface heights and slopes do not decorrelate. This results in a formula for the normalized cross section  $\sigma^\circ$  for the rough surface which must be expressed as a triple integral (TI). Simpler PO models can be obtained by assuming the rms surface slopes are small ( $\sigma/T < 1$ ). Still further simplifications for  $\sigma^\circ$  can be obtained by taking the high frequency geometrical optics (GO) limit. The various models for  $\sigma^\circ$  are compared for various angles of incidence  $\theta_i$  and scattering  $\theta_s$  as a function of surface roughness. In general, only the exact TI model accurately predicts enhanced em wave backscattering near the antispecular ( $\theta_s = -\theta_i$ ) direction. Of the various approximations for  $\sigma^\circ$ , the single integral PO  $F(\mu_{sp})$  model agrees best with the exact TI solution for most ranges of the parameters ( $\theta_i$ ,  $\theta_s$ ,  $\sigma$  and  $T$ ). In the examples shown here, GO also gives good agreement.

The physical mechanism responsible for the enhanced backscatter predicted by the PO TI model is not multiple scattering, because PO is based on a single scatter formalism. Here, it is diffuse backscatter from a sufficient number of facets with relatively large rms surface slopes. This is the reason why the TI model gave good agreement with the experimental results of Mendez and O'Donnell, where the rms slopes for the aluminum surface were relatively large. However, for the scattering from a rough gold surface reported by O'Donnell and Mendez<sup>2</sup>, the agreement between the theoretical triple integral model and the experimental data was not too good because the rms surface slopes were small ( $\sigma/T < 0.5$ ). O'Donnell and Mendez<sup>2</sup> claim that in this case the backscatter enhancement must be due to multiple scattering. Therefore, although multiple scattering may increase as the rms slope increases, a second mechanism comes into play for moderate and large slopes, that is, there are enough facets oriented to give a specular return in the backscatter direction.



The theoretical TI model will predict backscatter enhancement for a gold surface if  $\sigma/T > 0.8$ . Bahar<sup>17</sup> has observed backscatter enhancement at small rms surface slopes using the full wave solution, so that multiple scattering is not the only mechanism here. Bahar's observation of backscatter enhancement was more pronounced when a Pierson-Moskowitz<sup>18</sup> spectrum was used to describe the correlation properties of the surface, rather than a Gaussian spectrum. Bahar<sup>17</sup> claims that the Pierson-Moskowitz spectrum better fits the correlation properties of the surfaces measured by Mendez and O'Donnell.<sup>1,2</sup>

---

<sup>17</sup> Bahar, E. (1989), Private Communication.

<sup>18</sup> Brown, G. (1978) Backscatter from a Gaussian-distributed perfectly conducting rough surface, *IEEE Trans. on Antennas and Propagation*, 26(3):472-482.

## References

1. Mendez, E.R. and O'Donnell, K.A. (1987) Observation of depolarization and backscattering enhancement in light scattering from Gaussian random surfaces, *Optics Communications*, **61**(2):91-95.
2. O'Donnell, K.A. and Mendez, E.R. (1987) Experimental study of scattering from characterized random surfaces, *Journal Optical Society of America*, **4**:1194-1205.
3. Beckmann, P. and Spizzichino, A. (1963) *The Scattering of Electromagnetic Waves From Rough Surfaces*, Pergamon Press, New York.
4. Desanto, J.A. and Brown, G.S. (1986) Analytical techniques for multiple scattering from rough surfaces, E. Wolf, *Progress In Optics*, **XXIII**, Elsevier Science Publishers.
5. Ruck, G.T., Barrick, D.E., Stuart, W.D. and Krickbaum, C.T. (1970) *Radar Cross Section Handbook*, **2**, Plenum Press.
6. Brown, G.S. (1984) Application of the integral equation method of smoothing to random surface scattering, *IEEE Trans. on Antennas and Propagation*, **AP-32**(12):1308-1312.
7. Nieto-Vesperinas, M. and Garcia, N. (1981) A detailed study of the scattering of scalar waves from random rough surfaces, *Opt. Acta*, **28**:1651-1672.
8. Bahar, E. (1987) Review of the full wave solutions for rough surface scattering and depolarization: Comparisons with geometric and physical optics, perturbation and two-scale hybrid solutions, *J. Geophys. Res.*, **92**(C5):5209-5224.
9. Celli, V., Maraduden, A.A., Marvin, A.M. and McGurn, A.R. (1985) Some aspects of light scattering from a randomly rough metal surface, *J. Opt. Soc. America*, **A2**:2225.
10. McGurn, A.R., Maraduden, A.A. and Celli, V. (1985) Localization effects in the scattering of light from a randomly rough grating, *Phys. Rev.*, **B31**:4866.
11. Flood, W. (1987) Wave Propagation: Although Electromagnetics is a Mature Science, New Problems are Challenging the Theoreticians, R & D Roundup, *Microwaves and RF*, **65**.

12. Thorsos, E.I. and Ishimaru, A. (1988) An examination of the full-wave method for rough surface scattering, URSI Radio Science Session B/F-1, Jan. 1988, Univ. of Colorado, Boulder, CO.
13. Brown, G.S. (1988) Enhanced Backscatter from the Kirchhoff Approximation, Private Communication.
14. Papa, R.J. and Woodworth, M.B. (1988) *The numerical evaluation of a physical optics normalized cross section for a rough surface*, RADC-TR-87-280, ADA198919.
15. Papa, R.J. and Lennon, J.F. (1988) Conditions for the validity of physical optics in rough surface scattering, *IEEE Trans. on Antennas and Propagation*, **36**(5):647-650.
16. Born, M. and Wolf, E. (1959) *Principles of Optics*, Pergamon Press.
17. Bahar, E. (1989), Private Communication.
18. Brown, G. (1978) Backscatter from a Gaussian-distributed perfectly conducting rough surface, *IEEE Trans. on Antennas and Propagation*, **26**(3):472-482.



## *MISSION of Rome Air Development Center*

RADC plans and executes research, development, test and selected acquisition programs in support of Command, Control, Communications and Intelligence (C<sup>3</sup>I) activities. Technical and engineering support within areas of competence is provided to ESD Program Offices (POs) and other ESD elements to perform effective acquisition of C<sup>3</sup>I systems. The areas of technical competence include communications, command and control, battle management, information processing, surveillance sensors, intelligence data collection and handling, solid state sciences, electromagnetics, and propagation, and electronic, maintainability, and compatibility.